Title: Follistatin-like 3 mediates paracrine fibroblast activation by cardiomyocytes

Authors: Kalyani D. Panse[1], Leanne E. Felkin[1], Marina M. López-Olañeta[2], Jesús Gómez-Salinero[2], María Villalba[2], Lucía Muñoz[2], Kazuto Nakamura[3], Masayuki Shimano[3], Kenneth Walsh[3], Paul J.R. Barton[1,4], Nadia Rosenthal[1,5] and Enrique Lara Pezzi[1,2,*].

Affiliations: [1]Heart Science Centre, Imperial College London, Hill End Road, Middlesex UB9 6JH, United Kingdom; [2]Fundación Centro Nacional de Investigaciones Cardiovasculares, Melchor Fernandez Almagro, 3, 28029 Madrid, Spain; [3]Whitaker Cardiovascular Institute, Boston University Medical Campus, Boston, Massachusetts 02118, USA; [4]NIHR Cardiovascular Biomedical Research Unit, Royal Brompton and Harefield NHS Foundation Trust, London, United Kingdom; [5]Australian Regenerative Medicine Institute, Monash University, Melbourne, Australia.

***Correspondance:** Enrique Lara-Pezzi, Cardiovascular Development and Repair Department, Fundación Centro Nacional de Investigaciones Cardiovasculares, Melchor Fernandez Almagro, 3, 28029 Madrid, Spain. Tel.: +34-914531200, x3309. E-mail: elara@cnic.es

ABSTRACT

Follistatins are extracellular inhibitors of TGF-β family ligands including activin A, myostatin and bone morphogenetic proteins. Follistatin-like 3 (FSTL3) is a potent inhibitor of activin signalling and antagonises the cardioprotective role of activin A in the heart. FSTL3 expression is elevated in patients with heart failure and is upregulated in cardiomyocytes by hypertrophic stimuli, but its role in cardiac remodelling is largely unknown. Here we show that production of FSTL3 by cardiomyocytes contributes to the paracrine activation of cardiac fibroblasts, inducing changes in cell adhesion, promoting proliferation and increasing collagen production. We found that FSTL3 is necessary for this response and for the induction of cardiac fibrosis. However full activation requires additional factors and we identify CTGF as a FSTL3 binding partner in this process. Together our data unveil a novel mechanism of paracrine communication between cardiomyocytes and fibroblasts that may provide potential as a therapeutic target in heart remodelling.

INTRODUCTION

Initial compensation of the heart to increased systemic demands is provided in the form of cardiac hypertrophy, where individual cardiomyocytes grow in order to increase contractile function and reduce ventricular wall tension [1-3]. Physiological cardiac hypertrophy is commonly seen in response to exercise training or during pregnancy, where the increased workload is transitory and matched by preserved contractility [4]. In contrast, persistent hypertrophic growth due to arterial hypertension, aortic stenosis or regurgitation leads to pathological hypertrophy, fibrosis, heart remodelling and eventually contractile dysfunction and heart failure [2,5].

Cardiac structure is maintained by the extracellular matrix (ECM), which provides support for proper contractile function of the heart. The ECM is composed of fibrillar collagens (predominantly type I and type III), basement membrane components like fibronectin and laminin, proteoglycans and glucosaminoglycans [6]. Adaptation to myocardial stress induces a number of cellular and molecular alterations that lead to changes in the ECM composition and the collagen network as well as in the cardiac structure. During conditions of chronic hypertension and pressure overload, cardiac hypertrophy gradually decompensates and reactive interstitial fibrosis develops, increasing ventricular stiffness and progressively affecting contractility and diastolic chamber filling capacity [7-9]. It is becoming increasingly evident that heart remodelling as a result of hypertrophy and fibrosis is orchestrated by intercellular communication between cardiomyocytes and fibroblasts, both through direct contact and through paracrine mediators. However, these mechanisms are not well understood.

TGF-β is an example of such interaction. It is produced by different cell types in the heart and promotes both hypertrophy and fibrosis by activating distinct signalling pathways in fibroblasts and cardiomyocytes. Other members of the TGF-β family have also been widely implicated in the pathogenesis of heart failure. Activins are homodimeric cytokines that modulate diverse pathophysiological processes including inflammation and wound healing, cell proliferation, differentiation, metabolism, fibrosis and cardiac remodelling [10-12]. In the heart, Activin A has a protective role following myocardial infarction and reduces cardiac hypertrophy after pressure overload [13,14]. Activin signalling is inhibited by the follistatin family of proteins. Both Follistatin (FST) and Follistatin-like 3 (Fstl3/FLRG/FSRP)

can bind activin with high affinity and neutralise its action by preventing its binding to the activin receptors [15]. On the other hand, both activin and TGF-β are known to transciptionally regulate the expression of FST and FSTL3 through Smad proteins in what appears to be a negative feedback loop [16,17].

We have recently shown that FSTL3 expression is induced in the myocardium of heart failure patients and correlates with poor cardiac function and disease severity [18]. Interestingly, elevated FSTL3 expression in serum has also been reported in response to heavy resistance training in humans [19]. We found a similar increase in FSTL3 expression in rodent hearts subjected to ischemic injury, pressure overload induced hypertrophy or hypertrophy resulting from infusion of the β2 adrenergic agonist clenbuterol [13,14,20]. FSTL3 in the hypertrophic heart is mainly produced by cardiomyocytes and interferes with the beneficial effects of activin. Activin-mediated protection against ischemic injury was abrogated by FSTL3, and knock-out of Fstl3 in the heart resulted in smaller cardiac infarct size following ischemia-reperfusion injury [13]. In addition, we observed that inhibition of Activin A by FSTL3 induces cardiac hypertrophy in a mouse model of pressure overload. Cardiac-specific Fstl3 knockout mice displayed reduced hypertrophy, improved function and lower levels of interstitial fibrosis than wild type mice [14]. However the role of FSTL3 in cardiac fibrosis was not explored in depth.

Here we show that the role of FSTL3 in heart disease is more complex than previously anticipated. We investigated the transcriptome of cardiac-specific Fstl3 knockout myocardium and found that FSTL3 is necessary for full cardiac fibrosis to develop in response to pressure overload. We show that cardiomyocyte-derived FSTL3 promotes fibroblast proliferation and adhesion, and is necessary for paracrine activation of collagen production in fibroblasts. These findings may have important implications for the clinical management of cardiac fibrosis.

MATERIALS AND METHODS

Patients and Human Samples

Human myocardial samples were obtained from hearts isolated from transplanted end-stage heart failure patients and from control biopsies as previously described [21,22]. All the human samples used in this study conform to the Declaration of Helsinki.

Mice and surgeries

Fstl3 knockout (KO) mice and surgical procedures on these mice have been previously described [13,14]. Mice homozygous for a *Fstl3* allele containing two *lox*P sites flanking exons 3-5 ($Fstl3^{flox/flox}$) were crossed with α-myosin heavy chain (α-MHC)-Cre transgenic mice on a C57BL/6 background. Recombination by Cre leads to excision of *Fstl3* exons 3, 4 and 5 such that the progeny containing $Fstl3^{flox/flox}$ as well as α-MHC-Cre lack Fstl3 expression in post-natal cardiomyocytes.

Trans-aortic constriction (TAC) was performed in 6-8 week old *Fstl3* KO mice and wild type (WT) littermate controls. Prior to induction of anesthesia, all mice were given buprenorphine (0.25 mg/kg s.c.). General anesthesia was induced by inhalation of isofluorane (3-4% (v/v) in oxygen) and maintained at 1-1.5%. Following chest hair removal and disinfection, an upper chest midline skin incision followed by median sternotomy was performed to open the chest cavity. A loose suture (7-0 silk) was placed around the aorta and a 27 gauge blunted needle, between the right innominate artery and left common carotid artery. The suture was tightened to fully constrict the aorta and the needle was removed, thereby leading to partial constriction of the transverse aorta. The chest cavity, the muscle and skin layer were closed, disinfected and the animals were allowed to recover in a warm chamber. Analgesia (0.1 mg/kg buprenorphine) was given up to twice daily for 2-3 days following surgery. The efficiency of the procedure and cardiac function measurements on these mice were previously reported [14]. All studies were approved by the Institutional Animal Care and Use Committee of Boston University.

Neonatal rat cardiomyocyte and fibroblast isolation

Neonatal rat ventricular cardiomyocytes and fibroblasts were isolated as described by Toraason *et.al*. [23], with some modifications. Hearts from 1-4 day old rat pups were quickly excised and placed in ice-cold Ca^{2+} and Mg^{2+} free Hank's buffered salt solution (CMF – HBSS). Atria and surrounding connective tissue were removed, and the ventricles were minced into 1 mm^3 small pieces and digested with 50 μg/ml trypsin in 10 ml CMF-HBSS overnight at 4^{o}C. Trypsin was inactivated by adding 0.5 ml soybean trypsin inhibitor (Worthington Biochemical Corporation, USA) in CMF-HBSS and incubating at 37^{o}C in 5% CO_2 (v/v) for 20 min. Samples were then digested with 750 units collagenase (Worthington Biochemical Corporation, USA) in Leibovitz L-15 serum-free medium (Sigma-Aldrich, UK) in a shaking water bath at 37^{o}C for 30-45 min. Cells were dislodged by triturating the suspension 10 times using a 10 ml serological pipette, washed once with equilibrated L-15 medium and filtered through a 0.70 μm cell strainer. Cells were then centrifuged and resuspended in 25 ml complete medium (Dulbecco's Modified Eagle Medium (DMEM) containing 4500 mg/L glucose, 200 mM L-glutamine, 10% [v/v] fetal calf serum (FCS), 100 units/ml penicillin and 0.1 mg/ml streptomycin; all from Sigma-Aldrich). The cell mixture was sequentially pre-plated thrice for 30, 30 and 20 minutes and the adherent fibroblasts were cultured further in complete medium while cardiomyocytes were transferred to a separate tube after the third pre-plating. Cells were plated in type I fibronectin-coated dishes (1 μg/cm^2, Sigma-Aldrich). Cardiomyocytes obtained by this protocol routinely had a purity of 97-99%. Cardiac fibroblasts were allowed to multiply for 1 week, split 1:3, cultured for another week (P1) and passaged twice to remove contaminating endothelial cells. For experimental setup, both cardiomyocytes and fibroblasts were serum-starved overnight and incubated with 200 ng/ml FSTL3 (R&D Systems, USA) and/or 0.5 μg/ml CTGF (eBioscience) as indicated in each experiment. Mechanical stretch was applied using Flexcell FX-4000 Tension Plus system (Flexcell International Corporation, USA). Cells were plated on fibronectin or collagen-coated BioFlex plates for 2 days in complete medium and serum-starved for 24 hours prior to experiments. The plates were loaded on 25 mm cylindrical loading posts and 10% or 15% equibiaxial stretch was applied at a frequency of 0.6Hz for 24 hours.

Cell Proliferation, Adhesion, Migration and Collagen Production

To determine cell proliferation, cells were incubated in serum free medium for 24 h and then stimulated for 24 h with 200 ng/ml and/or 0.5 μg/ml CTGF in serum free medium. During the last 18 h of the stimulation, cells were grown in the presence of bromodeoxyuridine (BrdU) according to the BrdU detection kit's instructions (Millipore, UK). The amount of BrdU incorporated into the newly synthesized DNA was determined using an anti-BrdU antibody followed by an HRP-linked secondary antibody as previously described [24]. Cell adhesion was analysed as we previously reported [25]. Briefly, cells were incubated in the presence of 100 ng/ml FSTL3 for 24 h, washed and detached using 10 mM EDTA. Cells were resuspended in serum free medium and allowed to adhere to uncoated tissue culture dishes for different periods of time. After fixation in 2% glutaraldehyde cells were stained with crystal violet and quantified in the spectrophotometer at 540 nm. Cell migration was assayed using a Transwell device with 8 μm pore diameter [26]. A total of 10^5 fibroblasts were seeded onto the upper chamber of the device in serum-free medium. Cells were stimulated with 200 ng/ml FSTL3 for 1 h and then allowed to migrate towards the bottom chamber containing 2% FCS as a chemoattractant. After 6 h, cells in the bottom chamber were detached using trypsin and counted. Newly synthesized soluble collagen in the supernatant of fibroblast cell cultures was assayed using Sircol collagen assay (Biocolor Ltd., UK).

Microarrays and qRT-PCR

Total RNA was purified from myocardial tissue and cells using Trizol (Sigma-Aldrich) followed by RNAeasy (Qiagen, Netherlands) as previously described [27]. Whole transcriptome analysis was performed using the Gene 1.0 ST Array System (Affymetrix, Santa Clara, CA). Microarray data was analyzed using the GeneSpring GX software suite (Agilent Technologies, USA). After scanning, raw data in each chip was normalized to the 50^{th} percentile and to the median of the chip. Samples were then further normalized on a gene per gene basis to the values obtained for sham wild type hearts and gene lists were filtered for raw expression >50. Fold change lists comparing two conditions were generated using a cut-off value of 1.4-fold. For gene ontology (GO) analysis, the generated gene lists were compared to existing GO lists in GeneSpring as previously reported [20,24,28,29]. Only those GO lists showing a correlation *p*-value <0.01 with the studied gene list are shown.

Microarray results were validated by quantitative real-time PCR (qRT-PCR) using Taqman chemistry. Gene expression in all samples was normalized to values for 18S as previously described [30].

Yeast Two Hybrid

A yeast two-hybrid assay was performed using the HybriZAP-2.1 Two-Hybrid pre-digested vector kit (Stratagene) to identify *in vivo* protein interaction partners for FSTL3. Truncated FSTL3 was used as a bait to test interaction with target proteins expressed artificially in the yeast from a neonatal rat cardiomyocyte cDNA library. FSTL3 was cloned in frame with the yeast Gal4 DNA-binding domain (BD) while the library proteins were expressed as hybrid proteins with the Gal4 transcriptional activation domain (AD). Neither hybrid protein was capable of initiating activation of the reporter gene by itself. When a specific interaction took place between the bait and target protein, the Gal4 BD and AD co-localised and activated expression of the reporter gene histidine (*HIS3*). Colonies which were positive for the reporter were selected and analysed for the sequence of the encoded target protein. The yeast host strain YRG-2 is defective in uracil, histidine, adenine, lysine, tryptophan and leucine.

Immunoprecipitation and Western Blot

Cardiac fibroblasts were lysed in 1 ml cold lysis buffer containing 50 mM Tris–HCl, pH 7.5, 150 mM NaCl, 1.5 mM $MgCl_2$, 1 mM EGTA, 10 mM NaF, 1 mM Na_3VO_4, 1 µg/ml leupeptin, 1 mM PMSF and 1% Triton-X100. The lysate was kept on ice for 15 min. and pre-cleared using 50 µl protein A/G agarose beads (Santacruz Biotechnology, USA) by rotation at 4^oC for 1 h. Tubes were centrifuged at 2000 rpm at 4^oC for 5 min. and the supernatant was incubated with 4 µg goat polyclonal anti-CTGF immunoprecipitation antibody (Santacruz Biotechnology) or normal goat IgG (Santacruz Biotechnology) as control for 3 h at 4^oC with rotation. A total of 50 µl protein A/G agarose beads were added and tubes were incubated overnight at 4^oC. Samples were centrifuged at 2000 rpm at 4^oC for 5 min. and pellets were washed, resuspended in 100 µl 1X reducing loading buffer (Cell Signaling) and boiled at 95^oC for 5 min. The tubes were then kept on ice briefly and centrifuged at 2000 rpm at 4^oC for 5 minutes. The presence of FSTL3 and CTGF was detected using anti-FSTL3 antibody (R&D Systems) and anti-CTGF by western blot [28].

Statistical Analysis

Statistical analysis was carried out using Graphpad Prism. Data are expressed as mean ± standard error of the mean. Unpaired t-tests, one-way ANOVA and two-way ANOVA tests were used as indicated. $p<0.05$ was taken as significant.

RESULTS

Cardiac-specific Fstl3 KO mice show reduced expression of fibrotic markers

We have previously shown that genetically modified mice with cardiomyocyte-specific deletion of Fstl3 (KO) develop less hypertrophy and fibrosis in response to pressure overload [14]. In order to gain insight into the underlying mechanisms we explored the myocardial transcriptome of both KO and wild type (WT) mice 21 days after transaortic constriction (TAC) or a sham operation. In WT mice, microarray analysis showed increased expression (>1.4-fold) of heart failure markers, cytoskeleton encoding genes and genes related to cell adhesion and extracellular matrix (ECM) following pressure overload, paralleled by a decrease in genes associated with mitochondrial metabolism (Tables S1-S4). KO mice showed a similar trend, compared to knockout sham animals, although a weaker induction of ECM-related genes was detected and no clear pattern of down-regulated genes was observed (Tables S9-S12). Comparison between KO and WT mice under sham conditions revealed few differentially expressed genes, in agreement with our previous findings showing that FSTL3 is only induced in stressed cardiomyocytes [14,18]. However, following TAC KO hearts showed significantly lower overall ECM-related gene expression compared to WT (Tables S15, S16). It is interesting to note that around 50% of genes whose expression was reduced in knockout mice belonged to categories related to the extracellular matrix, rather than to growth or cytoskeleton. These results suggest that a major pathological role of FSTL3 in the heart is the regulation of fibrosis.

To validate these results we carried out qRT-PCR analysis on sham and hypertrophic hearts. We first analysed the expression of heart failure markers in these mice and found that WT mice showed a strong increase in ANP, BNP, α-skeletal actin and β-myosin heavy chain 21 days after TAC, which were significantly decreased in KO mice (Fig. S1), in agreement with the reduced hypertrophy observed in these mice and with experiments *in vitro* using FSTL3 siRNA [14]. Importantly, whereas no clear changes were found in the expression of inflammatory mediators (Fig. S2), KO mice expressed significantly lower levels of ECM genes and fibrosis markers. As shown in Figure 1, collagen I α1 (Col1a1) and collagen III α1 (Col3a1) mRNA were strongly induced after TAC in WT mice. Similarly, the mRNA

expressions of lysyl oxidase (Lox), an enzyme cross-linking collagen fibres into mature collagen (C) [31], and fibronectin-1, which is crucial for collagen deposition (D) [32], were also elevated in the WT hearts. In contrast, KO mice showed reduced expression of these markers following TAC, compared to WT, indicating reduced collagen deposition and fibrosis and validating the microarray results. Analysis of pro-fibrotic growth factors showed that mRNA and protein expression of both TGF- β1 and CTGF was also elevated after TAC in WT mice compared to sham operated hearts, but remained unchanged in KO hearts after TAC (Fig. 1E-1H).

Pressure-overload in the heart often leads to myocardial remodelling and progression to heart failure. Extracellular matrix components including matrix metalloproteinases (MMPs) and their tissue inhibitors (TIMPs) play an active role in this process [33]. In order to check if FSTL3 was involved in the regulation of these molecules, the expression of typical markers of myocardial remodelling was examined using qRT-PCR. As shown in Figure 2, the expression of MMP2 and MMP9 increased in WT hearts in response to pressure overload. In contrast, KO hearts showed attenuated expression of both. Expression of ADAM12 – a disintegrin and metalloprotease – followed a similar pattern and showed reduced expression in KO hearts compared to WT hearts after TAC (Fig. 2C). Furthermore, expression of the tissue inhibitor of MMPs TIMP1 was elevated in WT mice but not in KO hearts following TAC (Fig. 2D). Together, these results suggest that FSTL3 is necessary for ECM deposition and remodelling in the hypertrophic heart.

Fstl3 mediates paracrine activation of fibroblasts

Since deletion of Fstl3 in cardiac myocytes significantly reduced fibrosis after pressure overload, we explored the possibility that FSTL3 might be mediating paracrine activation of fibroblasts. To address this question, we cultured cardiac fibroblasts in the presence of conditioned medium from cardiomyocyte cultures subjected to stretch. As shown in Figure 3, stretching induced FSTL3 production by cardiomyocytes and conditioned medium derived from these cells significantly induced collagen release by fibroblasts (Fig. 3B). To determine the role of FSTL3 in this paracrine effect, we performed similar experiments in the presence of a neutralizing anti-FSTL3 or an isotype control antibody. As shown in Figure 3C, blockade of FSTL3 prevented collagen release from fibroblasts stimulated with conditioned medium form stressed cardiomyocytes. Of note, stretch had no effect on collagen expression in

cardiomyocytes themselves, ruling out the possibility that collagen was being released by these cells (Fig. S3). These results define FSTL3 as a paracrine mediator of fibroblast activation.

Fstl3 induces fibroblast proliferation and alters cell adhesion

Our data demonstrate that cardiac myocytes can activate fibroblasts and that FSTL3 is required for this effect. To determine if FSLT3 alone is sufficient to elicit this response we investigated the effect of exogenous FSTL3 protein on fibroblasts in terms of proliferation, adhesion, migration and collagen gene expression. Fibroblasts treated with FSTL3 alone induced a mild but significant increase in cell proliferation as measured by BrdU incorporation (Fig. 4A). We next explored its effects on fibroblast adhesion, since FSTL3 has previously shown to increase adhesion of hematopoietic progenitors to fibronectin [34]. We treated fibroblasts with FSTL3 for 24 h and allowed them to adhere to a culture dish for different periods of time. As shown in Fig. 4B, FSTL3 induced an increase in cell adhesion already at early time points. This effect was abolished if cells were detached with trypsin prior to the adhesion assay (data not shown), indicating that the action of FSTL3 is dependent on membrane proteins, likely integrins. Cell migration was measured using a Transwell device. Fibroblasts in the upper chamber were stimulated with FSTL3 and allowed to migrate towards the bottom chamber containing FCS as a chemoatractant. In contrast to cell adhesion, we detected no changes in cell migration (Fig. 4C). Similarly, no differences were found in collagen I expression in resting fibroblasts incubated with FSTL3 (Fig. 4D).

To test whether additional factors might be necessary for the action of FSTL3 on fibroblasts, mechanical stretch was applied to cultured cells. As shown in Figure 4E, Col1a1 expression was elevated when fibroblasts were stretched prior to FSTL3 stimulation, whereas stretch itself did not enhance collagen expression. Overall these data argue that FSTL3 acts to induce proliferation and adhesion but that other factors are required for full fibroblast activation.

Fstl3 interacts with CTGF

FSTL3 is believed to act, at least in part, through interaction with components of the TGF-β family such as myostatin, Activin or BMPs. However, there has been no systematic study on FSTL3 interacting factors, or of potential intracellular binding proteins in the heart. To address this issue we carried out a yeast two-hybrid assay using FSTL3 linked to the DNA binding domain of Gal4 as a bait for a rat cardiomyocyte cDNA library linked to the transcription activation domain of Gal4. A total of 156 clones were selected based on their activation of a reporter gene and identified by sequencing. After eliminating probable false positives in the form of mitochondrial, ribosomal and cloning vector targets as well as out-of-frame sequences, 110 likely targets were identified. As shown in Table S17, a number of targets identified were encoded in multiple individual clones, thereby indicating high likelihood of interaction with FSTL3. Interestingly, fibronectin 1 was encoded in 5 separate clones. This served as a positive control as interaction of FSTL3 with type I domains of fibronectin has been previously reported, although not in the heart [34]. A majority of 34 clones encoded syntenin, a cytoplasmic syndecan binding protein. The second most abundant gene found was connective tissue growth factor (CTGF), a well-known fibrotic marker. A number of targets such as granulin, EFEMP2, fibronectin, laminins, fibulins or fibrillins are components of the extracellular matrix (ECM) and basement membranes. Thus, it seems likely that FSTL3 may interact with ECM-associated proteins to potentiate its downstream effects.

From the collection of probable FSTL3 interaction partners, connective tissue growth factor (CTGF) seemed a most promising candidate due to its previously documented role in the regulation of cardiac hypertrophy and fibrosis [35-37]. To validate this interaction we immunoprecipitated CTGF from a cardiomyocyte lysate using an anti-CTGF antibody and observed co-immunoprecipitation of FSTL3 proteins by western blot (Fig. 5A). In order to test the functional consequences of this interaction we first investigated their effect on fibroblast proliferation either alone or in combination. As shown in Fig. 5B, both proteins enhanced cell proliferation on their own and showed a slightly stronger effect when combined. We next examined whether CTGF together with FSTL3 were sufficient to induce collagen expression by fibroblasts. We observed no significant differences in Col1a1 expression after stimulation with both proteins, either alone or in combination (Fig. 5C), suggesting that additional signals are necessary.

We have previously identified elevated myocardial FSTL3 as a feature of human patients with end-stage heart failure [21]. We examined the same patients for levels of CTGF

and found a strong positive correlation was found between FSTL3 and CTGF (Fig. 6D). This correlation was also observed between FSTL3 and another of its interactors, Fibronectin 1, as we previously reported [21].

DISCUSSION

Cardiac fibrosis is often seen as part of the remodelling response of the hypertrophied myocardium and many interventional studies have noted simultaneous reduction or increase in both cardiac hypertrophy and fibrosis. In contrast, other studies have reported differential regulation of hypertrophy and fibrosis. TGF-β triggers distinct signals in cardiomyocytes and fibroblasts to promote hypertrophy and fibrosis respectively [38]. Similarly, mice with constitutive active PI3K or dominant negative PI3K in the heart showed increased or decreased cardiac size respectively without any effect on fibrosis [39]. Cardiac specific Fstl3 KO mice displayed reduced interstitial collagen and cardiac remodelling which may be a direct effect of reduced hypertrophy following pressure overload [14]. However, microarray analysis in these mice suggested that FSTL3 may function mainly by modulation of extracellular matrix components rather than hypertrophic mediators. Moreover, cardiomyocytes being the main source of increased FSTL3 in the stressed heart suggested that FSTL3 may function through autocrine and/or paracrine actions on other cell types in the myocardium. This was further supported by *in vitro* observations demonstrating a necessary role for cardiomyocyte-derived FSTL3 in fibrosis development through paracrine actions.

Recently, a number of studies have focused on the function of paracrine factors in mediation of cardiac hypertrophy and fibrosis. For example,. Cardiomyocyte-derived TGF-β has been recognized to act on fibroblasts in the presence of angiotensin II to enhance collagen production and increase cell adhesion [40,41]. Furthermore, it was recently reported that paracrine action of TGF-β from cardiomyocytes is necessary for the protective effects of TGF-β type II receptor inhibition in the form of attenuated hypertrophy as well as fibrosis in response to pressure overload [38]. Similarly, IL-6 family cytokines have also been shown to play a paracrine role in fibrosis and cardiomyocyte hypertrophy. Pro-hypertrophic angiotensin II signalling induced IL-6, cardiotrohpin-1 (CT-1) and LIF expression in cardiac fibroblasts, which activated gp-130 signalling in cardiomyocytes to induce hypertrophic responses [42]. CT-1 stimulation was also sufficient to induce cardiac fibroblast growth and collagen synthesis and exhibited cooperation with endothelin-1/ET_A receptor signalling [43]. In this context, we show here that cardiomyocyte-derived FSTL3 induces paracrine fibroblast activation, promoting cell proliferation, adhesion and collagen production in conjunction with other factors. The reduction in interstitial fibrosis observed in cardiomyocyte-specific Fstl3

KO mice [14] together with the decreased expression of pro-fibrotic factors and ECM remodelling genes observed in these mice (Fig. 1 and 2) further reinforce the role of FSTL3 as a paracrine pro-fibrotic factor. Additionally, FSTL3 may also act on endothelial and vascular smooth muscle cells in the myocardium, as has been previously reported for FSTL1 [44,45]. Increased FSTL3 expression was detected in the endothelium of failing hearts [18], and may have adverse effects in the response to injury, possibly by inducing perivascular fibrosis.

The dependence of the paracrine action of FSTL3 on additional stretch-derived factors from the myocardium suggests a coordinated response of the heart undergoing remodelling. In this regard, endothelin-1 and angiotensin II have been described to be released by cardiac myocytes upon mechanical stretch [46,47]. Similar effects have been reported in neonatal rat cardiac fibroblasts subjected to mechanical loading and stimulation with IGF-1, in which increased expression of *α1* collagen type I mRNA was observed [48]. Many humoral factors and cytokines including angiotensin II, endothelin-1, TNF-α and TGF-β have been known to be secreted by mechanically loaded fibroblasts and are crucial to collagen synthesis and ECM remodelling [49-52]. Although the identity of the factors cooperating with FSTL3 remains as yet unknown, it is possible that a cell surface receptor on fibroblasts may only be expressed or morphologically exposed upon mechanical stretch. This regulation has been shown for surface integrins on fibroblasts, whose expression is changed in response to mechanical stimuli and which have been known to act as receptor complexes for mechanosensitive signal transduction [53].

Using a yeast two-hybrid approach we identified connective tissue growth factor (CTGF) among other FSTL3 interactors. Most of these were ECM-associated proteins involved in homeostasis, remodelling and structural integrity. In addition, our microarray analysis showed that most proteins from the ECM were downregulated in response to pressure overload in Fstl3 KO hearts compared to WT and we recently showed that FSTL3 expression correlates with fibrosis markers and mediators, like fibronectin 1 and CTGF, in patients with end-stage heart failure [21]. Together these results suggest that FSTL3 may act through these factors to mediate its effect on cardiac fibrosis and maybe also hypertrophy. Although CTGF interaction with FSTL3 did not alter collagen synthesis in fibroblasts, it was found to promote mild fibroblast proliferation and may thus be an important pro-fibrotic mechanism in the heart. Due to the modular structure of CTGF and its interaction with several extracellular signalling proteins as well as cell surface molecules, it is possible that

FSTL3 may use CTGF to sequester itself to specific cell surface proteins to act in a context-specific manner. A cardioprotective role of CTGF was recently demonstrated in a mouse model of ischemia-reperfusion injury in which CTGF reduced scar size and protected the myocardium from ischemic injury [54]. Whether the FSTL3-CTGF interaction may interfere with the cardioprotective actions of CTGF remains to be explored, but in a similar context we have previously shown that FSTL3 abolishes the cardioprotective effects of Activin A [13,14]. Although the molecular mechanism through which FSTL3 promotes fibroblast activation remains partially unknown and indeed a receptor for FSTL3 has so far not been found, our data suggest that it may contribute to fibrosis by acting as a co-factor of other pro-fibrotic molecules.

FSTL3 action on cardiomyocytes and fibroblasts and its role in their cross-talk represents an important target of therapeutic manipulation. In this regard, the action of FSTL3 from cardiomyocyte conditioned medium could be inhibited by the addition of a neutralising antibody. These have been recognized to be highly specific molecular tools to inhibit the action of important disease regulators. Antibody therapy against both TGF-β1 and TNF-α has been shown to effectively reduce cardiac fibrosis and progression to heart failure [55,56]. In this respect, FSTL3 inhibition by neutralising antibody may be used as an effective therapeutic strategy to minimize the harmful actions of FSTL3 on cardiomyocytes as well as fibroblasts, reducing the development of cardiac hypertrophy and fibrosis.

CLINICAL STATEMENT

There is increasing evidence that cardiomyocytes and fibroblasts communicate through different soluble mediators. However, the role and the identity of these mediators in cardiac fibrosis and the progression of heart disease are not well understood. This project was born out of an interesting clinical observation: the strong induction of FSTL3 expression in myocardial samples from heart failure patients [328]. Here we show that FSTL3 is secreted by mechanically stimulated cardiomyocytes to activate cardiac fibroblasts. Cardiomyocyte-specific knockout of Fstl3 considerably reduces cardiac fibrosis, further underlining the importance of FSTL3 as a paracrine fibrotic mediator. Our data suggest that FSTL3 is a clinically-relevant target whose inhibition may have therapeutic potential for the treatment and/or prevention of cardiac fibrosis, remodeling and heart failure.

ACKNOWLEDGEMENTS

This work was supported by a British Heart Foundation grant (PG/08/084/25827) to P.B., N.R. and E.L.P. In addition, PB was supported by Heart Research UK and by the National Institute for Health Research Cardiovascular Biomedical Research Unit at the Royal Brompton and Harefield NHS Foundation Trust and Imperial College. E.L.P. was supported by grants from the European Union (ERG-239158, ITN-289600), the Spanish Ministry of Science and Innovation (BFU2009-10016, CP08/00144) and the Regional Government of Madrid (S2010/BMD-2321 "Fibroteam").

REFERENCES

1. Spann JF, Bove AA, Natarajan G, Kreulen T (1980) Ventricular performance, pump function and compensatory mechanisms in patients with aortic stenosis. Circulation 62:576-582.

2. Grossman W, Jones D, Mclaurin LP (1975) Wall stress and patterns of hypertrophy in the human left ventricle. The Journal of Clinical Investigation 56:56-64.

3. Sasayama S, Ross J, Jr., Franklin D, Bloor CM, Bishop S, Dilley RB (1976) Adaptations of the left ventricle to chronic pressure overload. Circulation Research 38:172-178.

4. Pluim BM, Zwinderman AH, Van Der Laarse A, Van Der Wall EE (2000) The Athlete's Heart : A Meta-Analysis of Cardiac Structure and Function. Circulation 101:336-344.

5. Wikman-Coffelt J, Parmley W, Mason D (1979) The cardiac hypertrophy process. Analyses of factors determining pathological vs. physiological development. Circulation Research 45:697-707.

6. Scott-Burden T (1994) Extracellular Matrix: The Cellular Environment. Physiology 9:110-115.

7. Weber K, Janicki J, Shroff S, Pick R, Chen R, Bashey R (1988) Collagen remodeling of the pressure-overloaded, hypertrophied nonhuman primate myocardium. Circulation Research 62:757-765.

8. Norton GR, Woodiwiss AJ, Gaasch WH, Mela T, Chung ES, Aurigemma GP, Meyer TE (2002) Heart failure in pressure overload hypertrophy: The relative roles of ventricularremodeling and myocardial dysfunction. J Am Coll Cardiol 39:664-671.

9. Brower GL, Gardner JD, Forman MF, Murray DB, Voloshenyuk T, Levick SP, Janicki JS (2006) The relationship between myocardial extracellular matrix remodeling and ventricular function. European Journal of Cardio-Thoracic Surgery 30:604-610.

10. Xia Y, Schneyer AL (2009) The biology of activin: recent advances in structure, regulation and function. J Endocrinol 202:1-12.

11. Yndestad A, Ueland T, Oie E, Florholmen G, Halvorsen B, Attramadal H, Simonsen S, Froland SS et al (2004) Elevated levels of activin A in heart failure: potential role in myocardial remodeling. Circulation 109:1379-1385.

12. Mahmoudabady M, Mathieu M, Dewachter L, Hadad I, Ray L, Jespers P, Brimioulle S, Naeije R et al (2008) Activin-A, Transforming Growth Factor-[beta], and Myostatin Signaling Pathway in Experimental Dilated Cardiomyopathy. Journal of Cardiac Failure 14:703-709.

13. Oshima Y, Ouchi N, Shimano M, Pimentel DR, Papanicolaou KN, Panse KD, Tsuchida K, Lara-Pezzi E et al (2009) Activin A and Follistatin-Like 3 Determine the Susceptibility of Heart to Ischemic Injury. Circulation 120:1606-1615.

14. Shimano M, Ouchi N, Nakamura K, Oshima Y, Higuchi A, Pimentel DR, Panse KD, Lara-Pezzi E et al (2011) Cardiac Myocyte-specific Ablation of Follistatin-like 3 Attenuates Stress-induced Myocardial Hypertrophy. J Biol Chem 286:9840-9848.

15. Schneyer A, Schoen A, Quigg A, Sidis Y (2003) Differential binding and neutralization of activins A and B by follistatin and follistatin like-3 (FSTL-3/FSRP/FLRG). Endocrinology 144:1671-1674.

16. Bartholin L, Maguer-Satta V, Hayette S, Martel S, Gadoux M, Bertrand S, Corbo L, Lamadon C et al (2001) FLRG, an activin-binding protein, is a new target of TGFbeta transcription activation through Smad proteins. Oncogene 20:5409-5419.

17. Bartholin L, Maguer-Satta V, Hayette S, Martel S, Gadoux M, Corbo L, Magaud JP, Rimokh R (2002) Transcription activation of FLRG and follistatin by activin A, through Smad proteins, participates in a negative feedback loop to modulate activin A function. Oncogene 21:2227-2235.

18. Lara-Pezzi E, Felkin LE, Birks EJ, Sarathchandra P, Panse KD, George R, Hall JL, Yacoub MH et al (2008) Expression of follistatin-related genes is altered in heart failure. Endocrinology 149:5822-5827.

19. Willoughby DS (2004) Effects of heavy resistance training on myostatin mRNA and protein expression. Med Sci Sports Exerc 36:574-582.

20. Lara-Pezzi E, Terracciano C, Soppa G, Smolenski R, Felkin L, Yacoub M, Barton P (2009) A gene expression profile of the myocardial response to clenbuterol. J Cardiovasc Transl Res 2:191-197.

21. Felkin L, Lara-Pezzi E, Hall J, Birks E, Barton P (2011) Reverse remodelling and recovery from heart failure are associated with complex patterns of gene expression. J Cardiovasc Transl Res 4:321-331.

22. Birks E, George R (2010) Molecular changes occurring during reverse remodelling following left ventricular assist device support. J Cardiovasc Transl Res 3:635-642.

23. Toraason M, Luken ME, Breitenstein M, Krueger JA, Biagini RE (1989) Comparative toxicity of allylamine and acrolein in cultured myocytes and fibroblasts from neonatal rat heart. Toxicology 56:107-117.

24. Lara-Pezzi E, Winn N, Paul A, Mccullagh K, Slominsky E, Santini MP, Mourkioti F, Sarathchandra P et al (2007) A naturally occurring calcineurin variant inhibits FoxO activity and enhances skeletal muscle regeneration. J Cell Biol 179:1205-1218.

25. Lara-Pezzi E, Majano PL, Yáñez-Mo M, Gómez-Gonzalo M, Carretero M, Moreno-Otero R, Sanchez-Madrid F, Lopez-Cabrera M (2001) Effect of the hepatitis B virus HBx protein on integrin-mediated adhesion to and migration on extracellular matrix. J Hepatol 34:409-415.

26. Lara-Pezzi E, Gomez-Gaviro MV, Galvez BG, Mira E, Iniguez MA, Fresno M, Martinez-A C, Arroyo AG et al (2002) The hepatitis B virus X protein promotes tumor cell invasion by inducing membrane-type matrix metalloproteinase-1 and cyclooxygenase-2 expression. J Clin Invest 110:1831-1838.

27. Gómez-Gaviro MV, Scott CE, Sesay AK, Matheu A, Booth S, Galichet C, Lovell-Badge R (2012) Betacellulin promotes cell proliferation in the neural stem cell niche and stimulates neurogenesis. Proc Natl Acad Sci USA 109:1317-1322.

28. Felkin LE, Narita T, Germack R, Shintani Y, Takahashi K, Sarathchandra P, López-Olañeta MM, Gómez-Salinero JM et al (2011) Calcineurin splicing variant CnAβ1 improves cardiac function after myocardial infarction without inducing hypertrophy. Circulation 123:2838-2847.

29. Bochmann L, Sarathchandra P, Mori F, Lara-Pezzi E, Lazzaro D, Rosenthal N (2010) Revealing new mouse epicardial cell markers through transcriptomics. PLoS ONE 5:e11429.

30. Felkin LE, Lara-Pezzi E, George R, Yacoub MH, Birks EJ, Barton PJ (2009) Expression of extracellular matrix genes during myocardial recovery from heart failure following left ventricular assist device (LVAD) support. J Heart Lung Transplant 28:117-122.

31. Csiszar K (2001) Lysyl oxidases: a novel multifunctional amine oxidase family. Prog Nucleic Acid Res Mol Biol 70:1-32.

32. Mcdonald JA, Kelley DG, Broekelmann TJ (1982) Role of fibronectin in collagen deposition: Fab' to the gelatin-binding domain of fibronectin inhibits both fibronectin and collagen organization in fibroblast extracellular matrix. The Journal of Cell Biology 92:485-492.

33. Spinale FG (2002) Matrix Metalloproteinases: Regulation and Dysregulation in the Failing Heart. Circulation Research 90:520-530.

34. Maguer-Satta V, Forissier S, Bartholin L, Martel S, Jeanpierre S, Bachelard E, Rimokh R (2006) A novel role for fibronectin type I domain in the regulation of human hematopoietic cell adhesiveness through binding to follistatin domains of FLRG and follistatin. Exp Cell Res 312:434-442.

35. Matsui Y, Sadoshima J (2004) Rapid upregulation of CTGF in cardiac myocytes by hypertrophic stimuli: implication for cardiac fibrosis and hypertrophy. J Mol Cell Cardiol 37:477-481.

36. Hayata N, Fujio Y, Yamamoto Y, Iwakura T, Obana M, Takai M, Mohri T, Nonen S et al (2008) Connective tissue growth factor induces cardiac hypertrophy through Akt signaling. Biochem Biophys Res Commun 370:274-278.

37. Panek AN, Posch MG, Alenina N, Ghadge SK, Erdmann B, Popova E, Perrot A, Geier C et al (2009) Connective tissue growth factor overexpression in cardiomyocytes promotes cardiac hypertrophy and protection against pressure overload. PloS one 4:e6743.

38. Koitabashi N, Danner T, Zaiman AL, Pinto YM, Rowell J, Mankowski J, Zhang D, Nakamura T et al (2011) Pivotal role of cardiomyocyte TGF-β signaling in the murine pathological response to sustained pressure overload. The Journal of Clinical Investigation 121:2301-2312.

39. Shioi T, Kang PM, Douglas PS, Hampe J, Yballe CM, Lawitts J, Cantley LC, Izumo S (2000) The conserved phosphoinositide 3-kinase pathway determines heart size in mice. EMBO J 19:2537-2548.

40. Sarkar S, Vellaichamy E, Young D, Sen S (2004) Influence of cytokines and growth factors in ANG II-mediated collagen upregulation by fibroblasts in rats: role of myocytes. American journal of physiology Heart and circulatory physiology 287:H107-117.

41. Stawowy P, Margeta C, Blaschke F, Lindschau C, Spencer-Hänsch C, Leitges M, Biagini G, Fleck E et al (2005) Protein kinase C epsilon mediates angiotensin II-induced activation of β1-integrins in cardiac fibroblasts. Cardiovasc Res 67:50-59.

42. Sano M, Fukuda K, Kodama H, Pan J, Saito M, Matsuzaki J, Takahashi T, Makino S et al (2000) Interleukin-6 Family of Cytokines Mediate Angiotensin II-induced Cardiac Hypertrophy in Rodent Cardiomyocytes. Journal of Biological Chemistry 275:29717-29723.

43. Tsuruda T, Jougasaki M, Boerrigter G, Huntley BK, Chen HH, D'assoro AB, Lee SC, Larsen AM et al (2002) Cardiotrophin-1 Stimulation of Cardiac Fibroblast Growth: Roles for Glycoprotein 130/Leukemia Inhibitory Factor Receptor and the Endothelin Type A Receptor. CircRes 90:128-134.

44. Oshima Y, Ouchi N, Sato K, Izumiya Y, Pimentel DR, Walsh K (2008) Follistatin-like 1 is an Akt-regulated cardioprotective factor that is secreted by the heart. Circulation 117:3099-3108.

45. Ouchi N, Oshima Y, Ohashi K, Higuchi A, Ikegami C, Izumiya Y, Walsh K (2008) Follistatin-like 1, a secreted muscle protein, promotes endothelial cell function and revascularization in ischemic tissue through a nitric oxide synthesis-dependent mechanism. J Biol Chem.

46. Sadoshima J-I, Xu Y, Slayter HS, Izumo S (1993) Autocrine release of angiotensin II mediates stretch-induced hypertrophy of cardiac myocytes in vitro. Cell 75:977-984.

47. Yamazaki T, Komuro I, Kudoh S, Zou Y, Shiojima I, Hiroi Y, Mizuno T, Maemura K et al (1996) Endothelin-1 is involved in mechanical stress-induced cardiomyocyte hypertrophy. J Biol Chem 271:3221-3228.

48. Butt RP, Bishop JE (1997) Mechanical Load Enhances the Stimulatory Effect of Serum Growth Factors on Cardiac Fibroblast Procollagen Synthesis. Journal of Molecular and Cellular Cardiology 29:1141-1151.

49. Van Wamel AJET, Ruwhof C, Van Der Valk-Kokshoorn LEJM, Schriern PI, Van Der Laarse A (2001) The role of angiotensin II, endothelin-1 and transforming growth factor-β as autocrine/paracrine mediators of stretch-induced cardiomyocyte hypertrophy. Mol Cell Biochem 218:113-124.

50. Van Wamel AJET, Ruwhof C, Van Der Valk-Kokshoorn LJM, Schrier PI, Van Der Laarse A (2002) Stretch-induced paracrine hypertrophic stimuli increase TGF-β expression in cardiomyocytes. Mol Cell Biochem 236:147-153.

51. Yokoyama T, Sekiguchi K, Tanaka T, Tomaru K, Arai M, Suzuki T, Nagai R (1999) Angiotensin II and mechanical stretch induce production of tumor necrosis factor in cardiac fibroblasts. American Journal of Physiology - Heart and Circulatory Physiology 276:H1968-H1976.

52. Lindahl GE, Chambers RC, Papakrivopoulou J, Dawson SJ, Jacobsen MC, Bishop JE, Laurent GJ (2002) Activation of Fibroblast Procollagen α1(I) Transcription by Mechanical

Strain Is Transforming Growth Factor-β-dependent and Involves Increased Binding of CCAAT-binding Factor (CBF/NF-Y) at the Proximal Promoter. Journal of Biological Chemistry 277:6153-6161.

53. Chiquet M, Gelman L, Lutz R, Maier S (2009) From mechanotransduction to extracellular matrix gene expression in fibroblasts. Biochim Biophys Acta 1793:911-920.

54. Ahmed MS, Gravning J, Martinov VN, Von Lueder TG, Edvardsen T, Czibik G, Moe IT, Vinge LE et al (2011) Mechanisms of novel cardioprotective functions of CCN2/CTGF in myocardial ischemia-reperfusion injury. American Journal of Physiology - Heart and Circulatory Physiology 300:H1291-H1302.

55. Kadokami T, Frye C, Lemster B, Wagner CL, Feldman AM, Mctiernan CF (2001) Anti-Tumor Necrosis Factor-{alpha} Antibody Limits Heart Failure in a Transgenic Model. Circulation 104:1094-1097.

56. Kuwahara F, Kai H, Tokuda K, Kai M, Takeshita A, Egashira K, Imaizumi T (2002) Transforming Growth Factor-{beta} Function Blocking Prevents Myocardial Fibrosis and Diastolic Dysfunction in Pressure-Overloaded Rats. Circulation 106:130-135.

FIGURE LEGENDS

Figure 1. Cardiac-specific Fstl3 KO mice show reduced expression of fibrosis markers. Total RNA was isolated from cardiac samples following TAC or sham procedures and qRT-PCR was used to measure the myocardial mRNA expression of Col1a1 (**A**), Col3a1 (**B**), Lox (**C**), fibronectin-1 (**D**), TGF-β1 (**E**) and CTGF (**F**). Two-way ANOVA followed by Bonferroni post-tests were used to calculate statistical significance. **p<0.01, ***p<0.001 vs. WT Sham; ##p<0.01, ###p<0.001 vs. WT TAC. n = 3-6 per group. **G, H**, TGF-β and CTGF protein expression was analysed in wild type and Fstl3 KO mice by western blot. Total Akt was determined to show equal sample loading.

Figure 2. Reduced expression of markers of extracellular matrix remodelling in Fstl3 KO hearts. MMP2, MMP9, Adam12 and TIMP1 mRNA expression was analysed in ventricular samples from WT and Fstl3 KO hearts by qRT-PCR 3 weeks after TAC or sham operation. Two-way ANOVA followed by Bonferroni post-tests were used to calculate statistical significance. **p<0.01, ***p<0.001 vs. WT Sham; ##p<0.01, ###p<0.001 vs. WT TAC. n = 3-6 per group.

Figure 3. Mechanically stretched cardiomyocytes express FSTL3 that induces collagen production by fibroblasts. A, Neonatal rat ventricular cardiomyocytes were subjected to 10% equibiaxial stretch for 24 h and FSTL3 mRNA expression was measured by qRT-PCR. **B**, Conditioned medium from stretched cardiomyocytes was added to neonatal rat cardiac fibroblasts and newly formed collagen released to the medium was measured using a colorimetric collagen assay. Data are expressed as mean ± SEM. Unpaired t-tests were used to calculate the p values both in (A) and (B). **p<0.01, ***p<0.001 compared to 'no stretch' control samples. n = 6-7. **C**, Anti-Fstl3 neutralizing antibody or an isotype matched control IgG were added to conditioned medium from stretched cardiomyocytes and collagen release from fibroblasts was measured. Data are expressed as mean ± SEM. 2-way ANOVA followed by Bonferroni post-test was used to calculate the statistical significance. *p<0.05

for 10% stretch vs. no stretch; # $p < 0.05$ for anti-FSTL3 vs. control IgG at 10% stretch. n = 4.

Figure 4. FSTL3 enhances fibroblasts proliferation, adhesion and collagen expression. A, Neonatal cardiac fibroblasts were stimulated for 24 h with 200 ng/ml FSTL3 in serum-free medium and BrdU incorporation during the last 18 h was measured to determine cell proliferation. *p<0.05 FSTL3 vs control in unpaired t-test. n=4. **B**, Fibroblasts were incubated with 100 ng/ml FSTL3 for 24 h and allowed to adhere to an uncoated tissue-culture dish in stimulus-free medium for the indicated periods of time. Attached cells were fixed and stained with crystal violet and absorbance was measured at 540 nm. Data are expressed as mean ± SEM. 2-way ANOVA followed by Bonferroni post-test was used to calculate the statistical significance. *p<0.05, **<0.01 FSTL3 vs control. n = 3. **C**, Fibroblasts were plated on the upper chamber of transwell migration devices in serum-free medium, stimulated with 200 ng/ml FSTL3 and allowed to migrate to the lower chamber containing 2% FCS. After 6 h, cells in the bottom chamber were detached and counted. Data are expressed as mean ± SEM. **D**, Fibroblasts were treated with 200 ng/ml FSTL3 for 24 h and Col1a1 mRNA expression was measured by qRT-PCR. **E**, Fibroblasts were subjected to 15% equibiaxial stretch for 24 h and then stimulated with 200 ng/ml FSTL3 for another 24 h. Col1a1 mRNA expression was measured using qRT-PCR and expressed as mean fold induction ± SEM. 2-way ANOVA followed by Bonferonni post-test was used to calculate statistical significance. ***p<0.001 stretch vs. no stretch. ##p<0.01 for FSTL3 vs. control. n = 3.

Figure 5. FSTL3 interacts with CTGF. A, CTGF was immunoprecipitated from fibroblast cell lysate using anti-CTGF antibody and the bound proteins detected by western blot. **B**, Fibroblasts were stimulated for 24 h with 200 ng/ml FSTL3, 500 ng/ml CTGF or both in serum-free medium and BrdU incorporation during the last 18 h was measured to determine cell proliferation. *p<0.05 stimulus vs control, unpaired t-test. n=4. **C**, Cells were stimulated for 24 h as in (B) and Col1a1 mRNA expression was analysed by qRT-PCR. **D**, FSTL3 and CTGF expression was determined by qRT-PCR in myocardial samples from heart failure patients (n=18) and Spearman correlation between both factors was calculated.

Figure 6. Schematic of FSTL3 action in the heart. FSTL3 is secreted from cardiomyocytes following mechanical loading and acts in an autocrine manner to induce cardiomyocyte hypertrophy. In coordination with unknown stretch-induced factors, FSTL3 acts in a paracrine manner on fibroblasts to promote collagen synthesis. In addition, FSTL3 interacts with CTGF to enhance fibroblast proliferation. Together these results suggest a role of FSTL3 in paracrine fibroblast activation.

Figure 1
Click here to download high resolution image

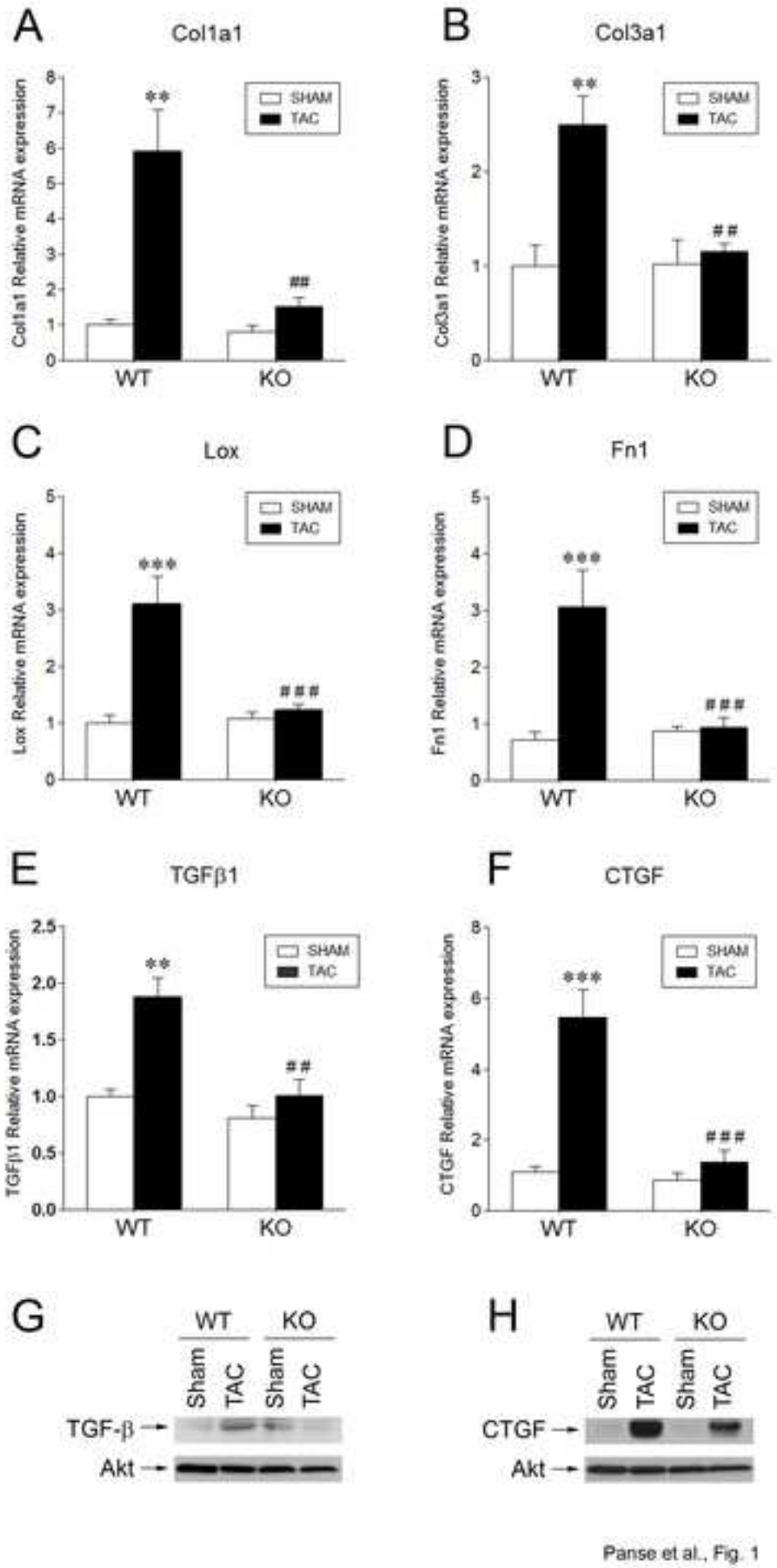

Panse et al., Fig. 1

Figure 2
Click here to download high resolution image

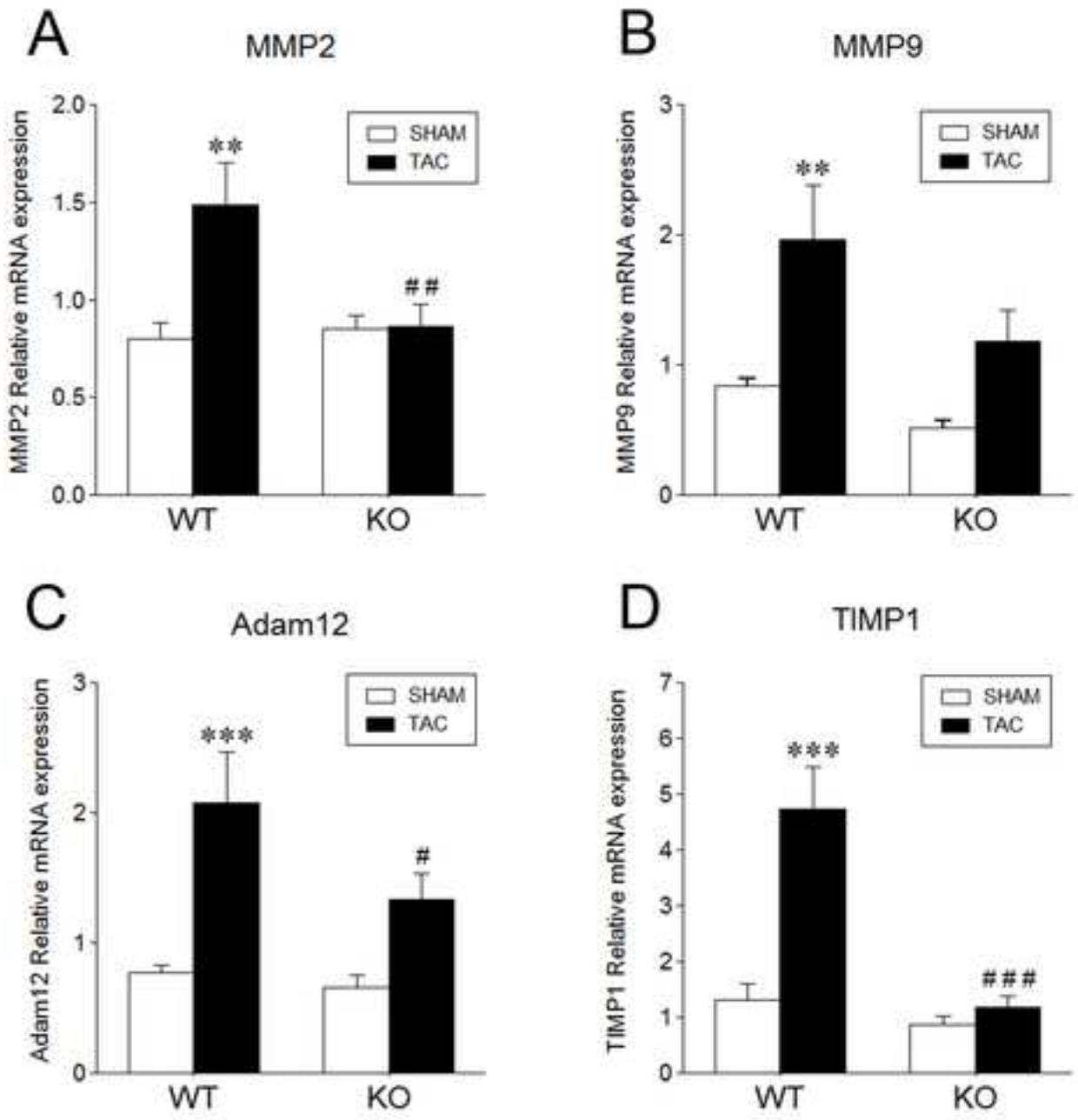

Panse et al., Fig. 2

Figure 3
Click here to download high resolution image

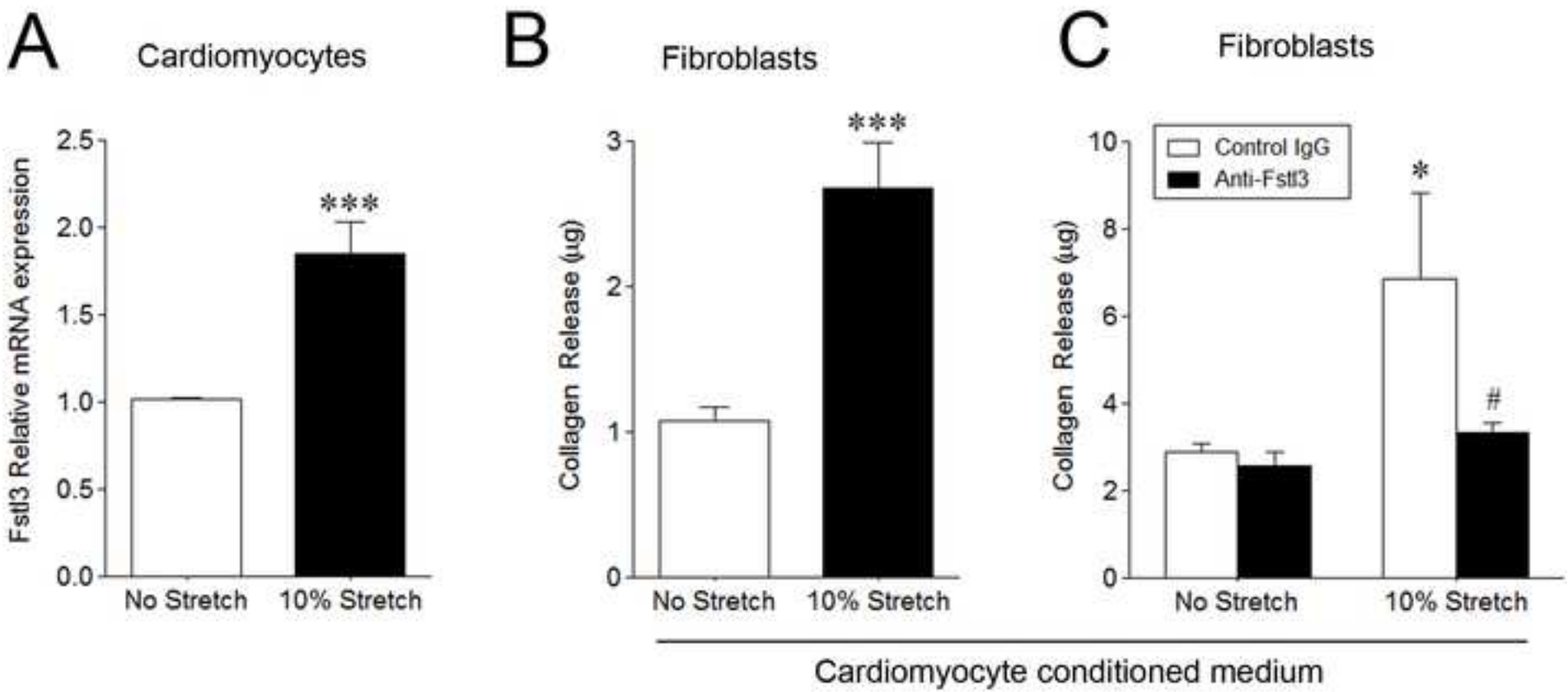

Panse et al., Fig. 3

Figure 4
Click here to download high resolution image

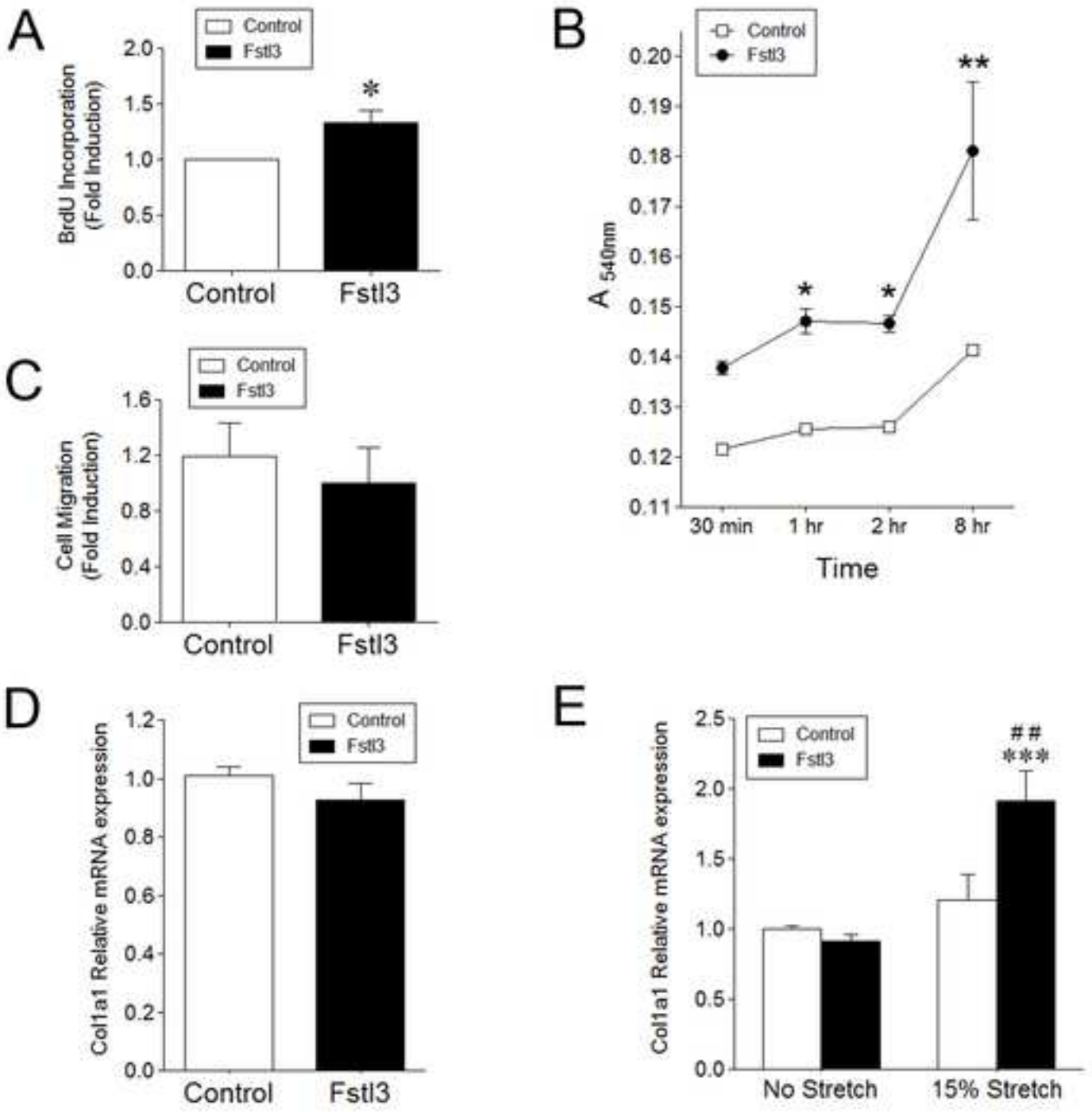

Panse et al., Fig. 4

Figure 5
Click here to download high resolution image

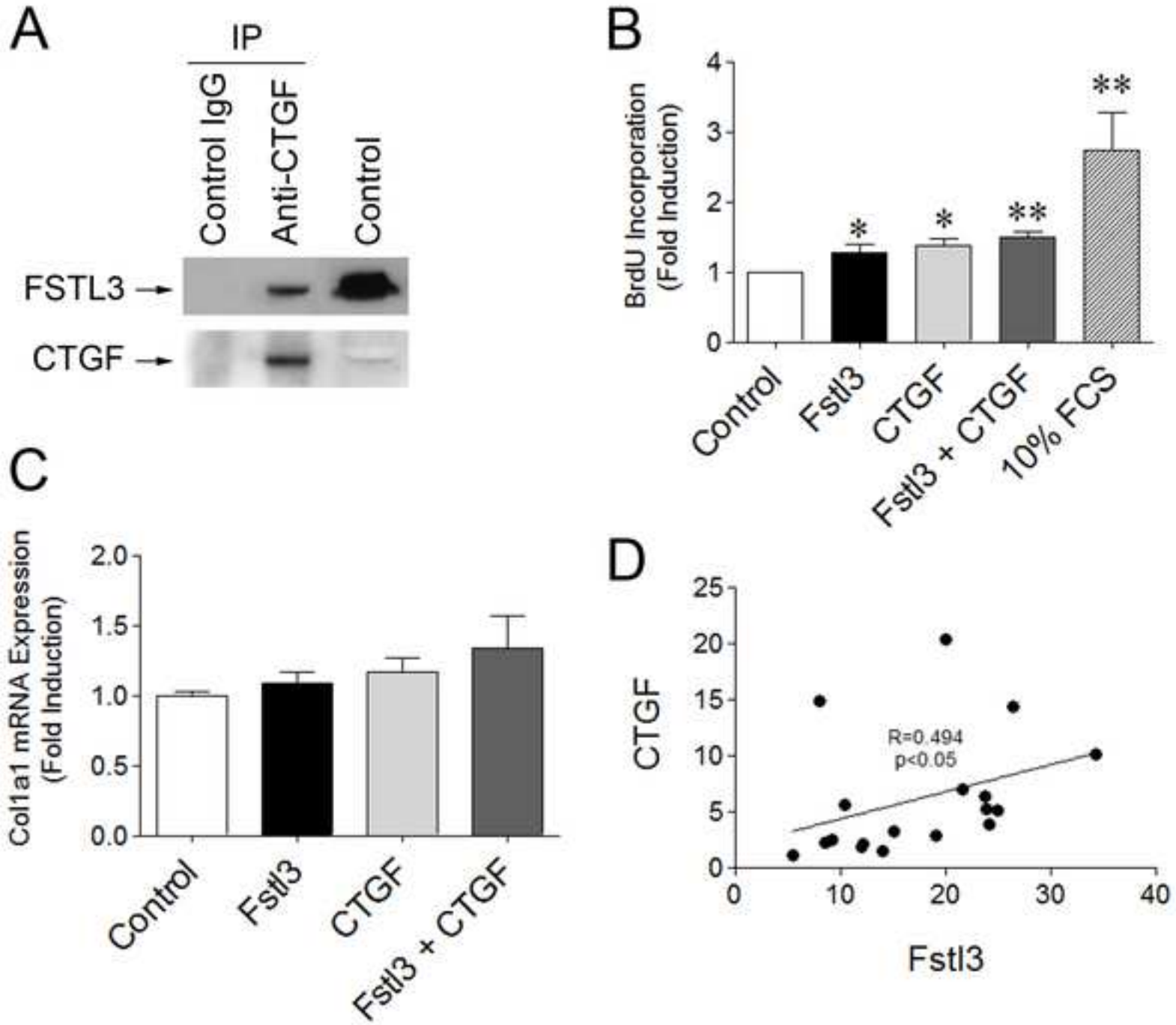

Panse et al., Fig. 5

Figure 6
Click here to download high resolution image

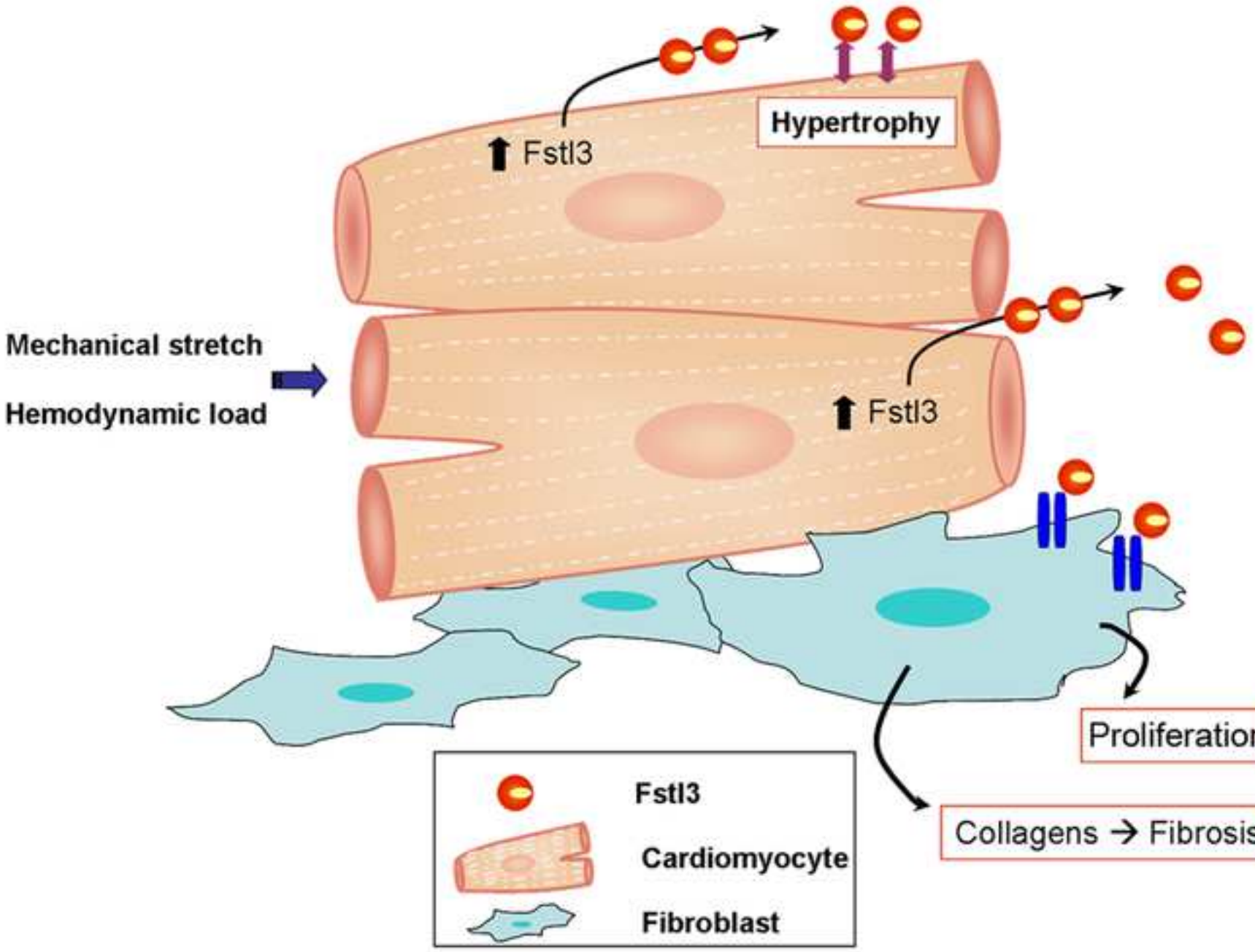

Panse et al., Fig. 6

SUPPLEMENTAL MATERIAL

FIGURE LEGENDS

Figure S1. Cardiac-specific Fstl3 KO mice show reduced expression of heart failure markers. Total RNA was isolated from cardiac samples following TAC or sham procedures and qRT-PCR was used to measure the myocardial mRNA expression of ANP/ANF (**A**), BNP (**B**), α-skeletal actin/Acta1 (**C**) and β-myosin heavy chain/Myh7 (**D**). Two-way ANOVA followed by Bonferroni post-tests were used to calculate statistical significance. **p<0.01, ***p<0.001 vs. WT Sham; #p<0.05, ##p<0.01, ###p<0.001 vs. WT TAC. n = 3-6 per group.

Figure S2. Expression of inflammation markers in Fstl3 KO hearts. mRNA expression of cytokines IL-1β and IL6, chemokine CCL5/Rantes and the macrophage marker CD68 was analysed in ventricular samples from WT and Fstl3 KO hearts by qRT-PCR 3 weeks after TAC or sham operation. Two-way ANOVA followed by Bonferroni post-tests were used to calculate statistical significance. **p<0.01, vs. WT Sham. n = 3-6 per group.

Figure S3. Mechanical stretched does not induce collagen expression in cardiomyocytes. **A**, Neonatal rat ventricular cardiomyocytes were subjected to 10% equibiaxial stretch for 24 h and Col1a1 and Col3a1 mRNA expression was measured by qRT-PCR. Data are expressed as mean ± SEM. Unpaired t-tests were used to calculate the p values. **p<0.01 compared to 'no stretch' control samples. n = 6-7.

SUPPLEMENTAL TABLES

Tables S1-S16. Microarray analysis of cardiac hypertrophy. RNA extracted from WT and KO hearts 21 days after transaortic constriction (TAC) or Sham operation was analyzed by microarray as described in materials and methods. Odd number tables contain lists of genes whose expression changes after >1.4-fold, between the sample groups indicated in the title. Even number tables contain the Gene Ontology analysis of the preceding gene list.

Table S17. Yeast two-hybrid analysis of FSTL3 interacting proteins. FSTL3 was used as a bait to identify possible interacting proteins expressed in yeast from a neonatal rat cardiomyocyte cDNA library. After eliminating probable false positives in the form of mitochondrial, ribosomal and cloning vector targets as well as out-of-frame sequences, 110 likely targets were identified. The number of clones that encoded each of them (Number of hits) is listed.

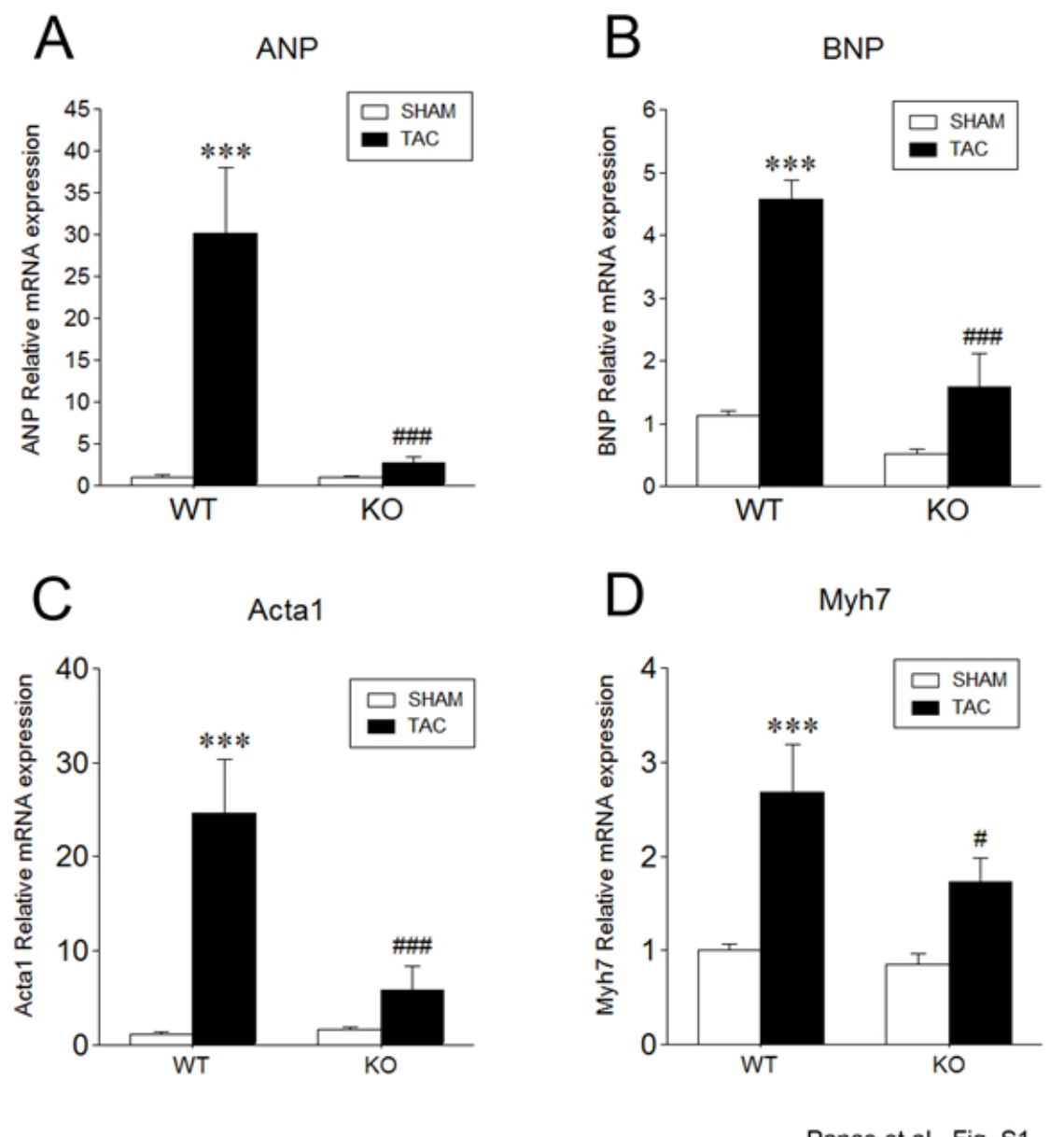

Panse et al., Fig. S1

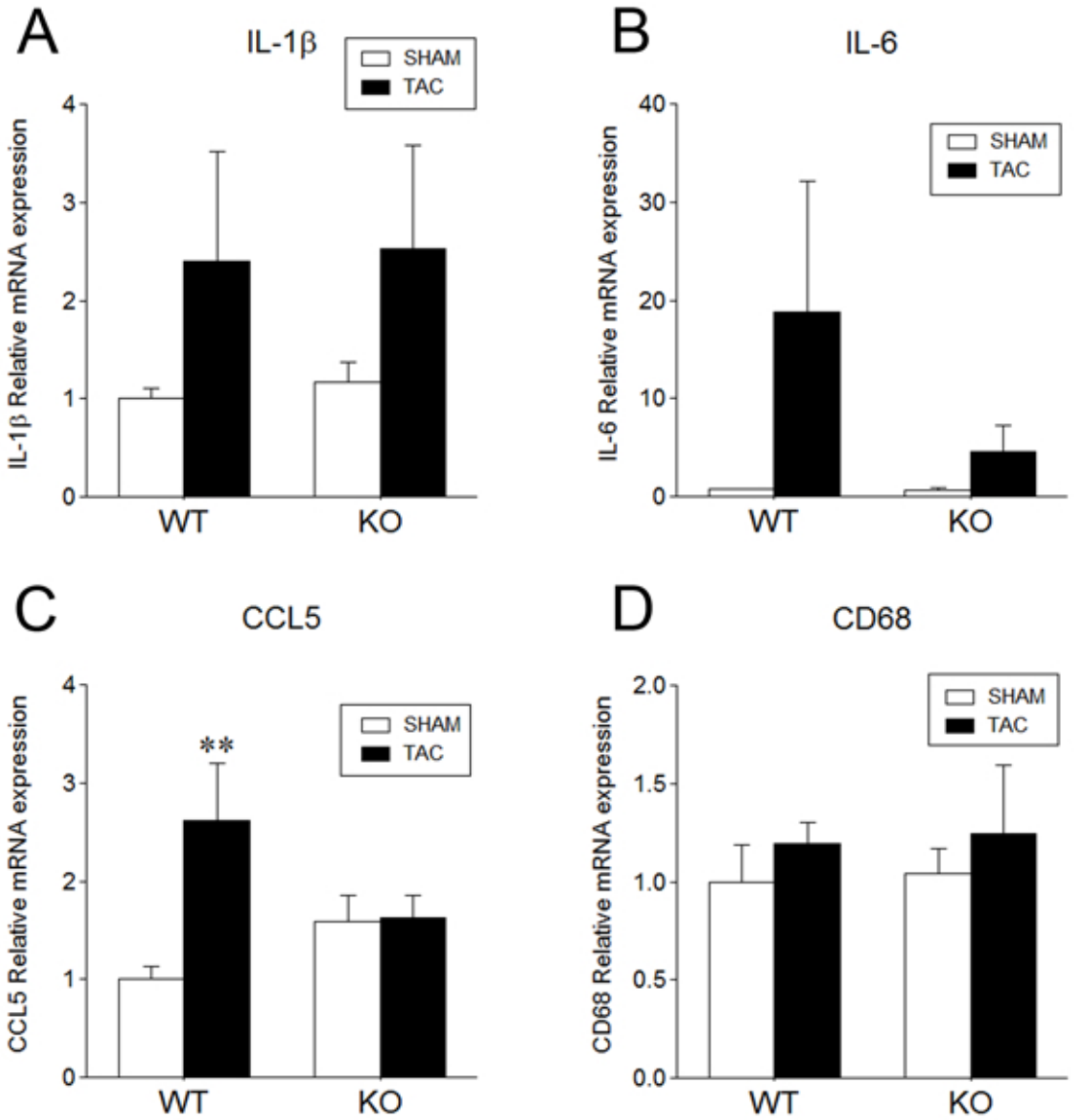

Panse et al., Fig. S2

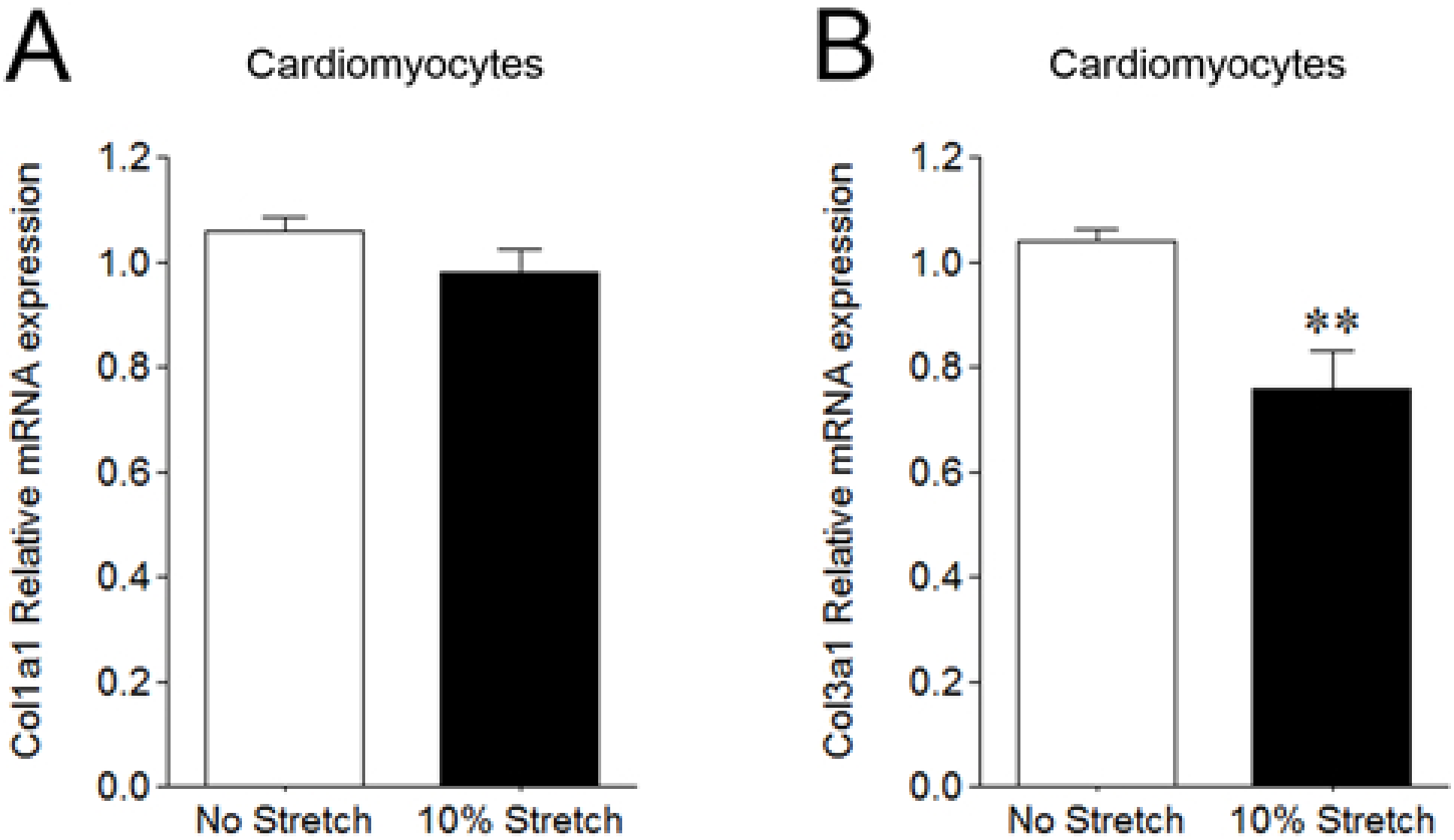

Panse et al., Figure S3

Supplemental Table 1 - WT TAC > WT Sham			
Affy ID	**Fold**	**Gene symbol**	**Description**
10398075	10.001	Serpina3n	serine (or cysteine) peptidase inhibitor, clade A, member 3N
10598976	7.667	Timp1	tissue inhibitor of metalloproteinase 1
10492021	7.584	Postn	periostin, osteoblast specific factor
10419934	6.169	Myh7	myosin, heavy polypeptide 7, cardiac muscle, beta
10358476	6.032	Prg4	proteoglycan 4 (megakaryocyte stimulating factor, articular superficial zone protein)
10586357	5.534	Cilp	cartilage intermediate layer protein, nucleotide pyrophosphohydrolase
10541496	4.826	Mfap5	microfibrillar associated protein 5
10481627	4.813	Lcn2	lipocalin 2
10582592	4.735	Acta1	actin, alpha 1, skeletal muscle
10440091	4.726	Col8a1	collagen, type VIII, alpha 1
10510265	4.572	Nppa	natriuretic peptide precursor type A
10401527	4.562	Ltbp2	latent transforming growth factor beta binding protein 2
10574023	4.359	Mt2	metallothionein 2
10376778	3.757	Mfap4	microfibrillar-associated protein 4
10417212	3.732	Itgbl1	integrin, beta-like 1
10355403	3.512	Fn1	fibronectin 1
10416181	3.506	Stc1	stanniocalcin 1
10462442	3.407	Il33	interleukin 33
10435641	3.232	Fstl1	follistatin-like 1
10534667	3.207	Serpine1	serine (or cysteine) peptidase inhibitor, clade E, member 1
10484307	3.194	Frzb	frizzled-related protein
10517213	3.075	Cnksr1	connector enhancer of kinase suppressor of Ras 1
10513739	3.055	Tnc	tenascin C
10572897	3.031	Hmox1	heme oxygenase (decycling) 1
10478048	2.986	Lbp	lipopolysaccharide binding protein
10542355	2.885	Emp1	epithelial membrane protein 1
10513208	2.864	Svep1	sushi, von Willebrand factor type A, EGF and pentraxin domain containing 1
10380419	2.854	Col1a1	collagen, type I, alpha 1
10554752	2.840	Nox4	NADPH oxidase 4
10424140	2.801	Col14a1	collagen, type XIV, alpha 1
10359851	2.763	Uck2	uridine-cytidine kinase 2
10388430	2.638	Serpinf1	serine (or cysteine) peptidase inhibitor, clade F, member 1
10536220	2.534	Col1a2	collagen, type I, alpha 2
10586865	2.515	Aldh1a2	aldehyde dehydrogenase family 1, subfamily A2
10416215	2.427	Loxl2	lysyl oxidase-like 2
10475517	2.417	AA467197	expressed sequence AA467197
10573979	2.336	Gnao1	guanine nucleotide binding protein, alpha O
10510260	2.319	Nppb	natriuretic peptide precursor type B
10463070	2.245	Entpd1	ectonucleoside triphosphate diphosphohydrolase 1
10450242	2.219	C4b///C4a	complement component 4B (Childo blood group)///complement component 4A (Rodgers blood grou
10359849	2.215	Uck2	uridine-cytidine kinase 2
10346015	2.210	Col3a1	collagen, type III, alpha 1
10582275	2.181	Slc7a5	solute carrier family 7 (cationic amino acid transporter, y+ system), member 5
10409464	2.176	Dbn1	drebrin 1
10401841	2.109	Dio2	deiodinase, iodothyronine, type II
10489878	2.097	Ptgis	prostaglandin I2 (prostacyclin) synthase
10374083	2.079	Aebp1	AE binding protein 1
10434698	2.075	Fetub	fetuin beta
10472426	2.061	Xirp2	xin actin-binding repeat containing 2
10523175	2.044	Ereg	epiregulin
10360764	2.032	Enah	enabled homolog (Drosophila)
10464761	2.031	Syt12	synaptotagmin XII
10461721	2.018	Mpeg1	macrophage expressed gene 1
10407481	2.004	Pfkp	phosphofructokinase, platelet
10429128	2.002	Sla	src-like adaptor
10562192	1.990	Fxyd5	FXYD domain-containing ion transport regulator 5
10572398	1.974	Crlf1	cytokine receptor-like factor 1
10467191	1.961	Ankrd1	ankyrin repeat domain 1 (cardiac muscle)
10600169	1.950	Bgn	biglycan

Supplemental Table 2 - GO: WT TAC > WT Sham

GO ID	GO ACCESSION	GO Term	p-value	corrected p-value	Count in Selection	% Count in Selection	Count in Total	% Count in Total
3394	GO:0005576	extracellular region	1.05E-15	1.36E-11	46	51.11111	1688	7.7477393
12843	GO:0031012	extracellular matrix	6.02E-15	3.91E-11	20	22.222221	292	1.3402488
3396	GO:0005578	proteinaceous extracellular matrix	2.45E-13	1.06E-09	18	20	274	1.2576307
18811	GO:0044420	extracellular matrix part	2.23E-12	7.24E-09	6	6.6666665	87	0.3993207
18812	GO:0044421	extracellular region part	9.11E-11	2.36E-07	20	22.222221	760	3.4883187
3351	GO:0005488	binding	8.26E-08	1.78E-04	58	64.44444	11058	50.75504
3365	GO:0005515|GO:0045308	protein binding	3.50E-07	6.49E-04	51	56.666668	5545	25.450956
4579	GO:0007015	actin filament organization	6.71E-07	8.71E-04	5	5.5555553	42	0.1927755
6431	GO:0009611|GO:0002245	response to wounding	5.57E-07	8.71E-04	1	1.1111112	359	1.6477716
25388	GO:0065008	regulation of biological quality	6.09E-07	8.71E-04	6	6.6666665	944	4.332859
3205	GO:0005201	extracellular matrix structural constituent	8.35E-07	9.85E-04	3	3.3333333	24	0.11015743
3420	GO:0005604	basement membrane	9.30E-07	0.001005622	6	6.6666665	70	0.32129252
5391	GO:0008360|GO:0045788|GO:0045789	regulation of cell shape	1.94E-06	0.001930834	6	6.6666665	50	0.22949465
11860	GO:0022603	regulation of anatomical structure morphogenesis	2.32E-06	0.002150899	6	6.6666665	114	0.52324784
4699	GO:0007155	cell adhesion	2.98E-06	0.002413551	14	15.555555	603	2.7677054
11867	GO:0022610	biological adhesion	2.98E-06	0.002413551	14	15.555555	603	2.7677054
11976	GO:0030029	actin filament-based process	3.74E-06	0.002855842	8	8.888889	162	0.7435627
2128	GO:0003779	actin binding	6.50E-06	0.004440153	11	12.222222	271	1.243861
11861	GO:0022604	regulation of cell morphogenesis	6.32E-06	0.004440153	6	6.6666665	61	0.2799835
6425	GO:0009605	response to external stimulus	9.40E-06	0.005808385	2	2.2222223	589	2.703447
8183	GO:0015629	actin cytoskeleton	1.10E-05	0.006480557	5	5.5555553	185	0.8491302
11983	GO:0030036	actin cytoskeleton organization and biogenesis	1.60E-05	0.008663518	7	7.7777777	148	0.6793042

Supplemental Table 3 - WT TAC < WT Sham			
Affy ID	**Fold**	**Gene symbol**	**Description**
10580635	7.043	Ces3	carboxylesterase 3
10598064	3.423		
10441794	3.019	Mrgprh	MAS-related GPR, member H
10598062	3.008		
10511363	2.946	Penk	preproenkephalin
10598018	2.486		
10386197	2.382	2210407C18Rik	RIKEN cDNA 2210407C18 gene
10602385	2.301	Pfkfb1	6-phosphofructo-2-kinase/fructose-2,6-biphosphatase 1
10579958	2.242	Il15	interleukin 15
10397763	2.238	9030617O03Rik	RIKEN cDNA 9030617O03 gene
10398824	2.209	A530016L24Rik	RIKEN cDNA A530016L24 gene
10534085	2.147	Phkg1	phosphorylase kinase gamma 1
10409999	2.119	Fbp2	fructose bisphosphatase 2
10462303	2.106	Kcnv2	potassium channel, subfamily V, member 2
10574488	2.055	Pdp2	pyruvate dehyrogenase phosphatase catalytic subunit 2
10433403	2.049	A2bp1	ataxin 2 binding protein 1
10468113	2.023	Kcnip2	Kv channel-interacting protein 2
10413381	2.018	Dnahc12///Asb14	dynein, axonemal, heavy chain 12///ankyrin repeat and SOCS box-containing 14
10436095	1.981	Retnla	resistin like alpha
10536611	1.980	Kcnd2	potassium voltage-gated channel, Shal-related family, member 2
10422028	1.971	Tbc1d4	TBC1 domain family, member 4
10536697	1.940	Asb15	ankyrin repeat and SOCS box-containing 15
10547153	1.936	Alox5	arachidonate 5-lipoxygenase
10369806	1.897	1700040L02Rik	RIKEN cDNA 1700040L02 gene
10537712	1.869	Gstk1	glutathione S-transferase kappa 1
10419525	1.853	A930018M24Rik	RIKEN cDNA A930018M24 gene
10480459	1.851	Hnmt	histamine N-methyltransferase
10428619	1.849	Enpp2	ectonucleotide pyrophosphatase/phosphodiesterase 2
10396079	1.842	Klhdc1	kelch domain containing 1
10357965	1.832	Lgr6	leucine-rich repeat-containing G protein-coupled receptor 6
10454683	1.815	Pkd2l2	polycystic kidney disease 2-like 2
10352133	1.813	Efcab2	EF-hand calcium binding domain 2
10598077	1.806		
10603746	1.789	Maob	monoamine oxidase B
10348906	1.772	Gm6086	predicted gene 6086
10598023	1.771		
10539143	1.770	Retsat	retinol saturase (all trans retinol 13,14 reductase)
10415279	1.758	Fitm1	fat storage-inducing transmembrane protein 1
10386020	1.758	Slc36a2	solute carrier family 36 (proton/amino acid symporter), member 2
10455146	1.744	3222401L13Rik	RIKEN cDNA 3222401L13 gene
10463704	1.735	As3mt	arsenic (+3 oxidation state) methyltransferase
10344725	1.728	Adhfe1	alcohol dehydrogenase, iron containing, 1
10422962	1.727	1110020G09Rik	RIKEN cDNA 1110020G09 gene
10377245	1.717	Dhrs7c	dehydrogenase/reductase (SDR family) member 7C
10606436	1.713	Hmgn5	high-mobility group nucleosome binding domain 5
10545001	1.697	Ppm1k	protein phosphatase 1K (PP2C domain containing)
10596718	1.696	Slc38a3	solute carrier family 38, member 3
10503484	1.679	Fam82b	family with sequence similarity 82, member B
10474361	1.638	Mpped2	metallophosphoesterase domain containing 2
10433177	1.630	Gm9108	predicted gene 9108
10438017	1.627	Fgd4	FYVE, RhoGEF and PH domain containing 4
10601878	1.623	Tceal1	transcription elongation factor A (SII)-like 1
10466903	1.621	4430402I18Rik	RIKEN cDNA 4430402I18 gene
10409737	1.620	Agtpbp1	ATP/GTP binding protein 1
10542834	1.619		
10348889	1.614	D2hgdh	D-2-hydroxyglutarate dehydrogenase
10589368	1.613	Plxnb1	plexin B1
10517600	1.610	Pink1	PTEN induced putative kinase 1
10409118	1.610	Wnk2	WNK lysine deficient protein kinase 2

10547410	1.609	LOC100048600///Erc1	ELKS/RAB6-interacting/CAST family member 1
10456699	1.608	Acaa2	acetyl-Coenzyme A acyltransferase 2 (mitochondrial 3-oxoacyl-Coenzyme A thiolase)
10569331	1.602	Gm14492	predicted gene 14492
10592061	1.598	Kcnj5	potassium inwardly-rectifying channel, subfamily J, member 5
10382321	1.586	Kcnj2	potassium inwardly-rectifying channel, subfamily J, member 2
10494388	1.585	Hist2h2be	histone cluster 2, H2be
10574350	1.582	Mmp15	matrix metallopeptidase 15
10402117	1.582	Rps6ka5	ribosomal protein S6 kinase, polypeptide 5
10368720	1.578	Slc16a10	solute carrier family 16 (monocarboxylic acid transporters), member 10
10360053	1.576	Pcp4l1	Purkinje cell protein 4-like 1
10587534	1.575	Bckdhb	branched chain ketoacid dehydrogenase E1, beta polypeptide
10494114	1.557	Selenbp1///Selenbp2///LOC	selenium binding protein 2///selenium binding protein 1
10423505	1.555	Cmbl	carboxymethylenebutenolidase-like (Pseudomonas)
10513692	1.550	Whrn	whirlin
10529082	1.548	Gtf3c2///Mpv17	general transcription factor IIIC, polypeptide 2, beta///MpV17 mitochondrial inner membrar
10497862	1.548	Trpc3	transient receptor potential cation channel, subfamily C, member 3
10478145	1.545	Ppp1r16b	protein phosphatase 1, regulatory (inhibitor) subunit 16B
10575363	1.543	Zfp612	zinc finger protein 612
10420935	1.541	Ephx2	epoxide hydrolase 2, cytoplasmic
10533504	1.538	Ift81	intraflagellar transport 81 homolog (Chlamydomonas)
10411532	1.529	Mccc2	methylcrotonoyl-Coenzyme A carboxylase 2 (beta)
10530819	1.526	Hopx	HOP homeobox
10509204	1.525	Tcea3	transcription elongation factor A (SII), 3
10550638	1.517	Rtn2	reticulon 2 (Z-band associated protein)
10406482	1.517	Ccnh	cyclin H
10595205	1.517	2410127L17Rik	RIKEN cDNA 2410127L17 gene
10401473	1.516	Aldh6a1	aldehyde dehydrogenase family 6, subfamily A1
10398751	1.511	Zfyve21	zinc finger, FYVE domain containing 21
10445214	1.510	Mut	methylmalonyl-Coenzyme A mutase
10424559	1.507	Khdrbs3	KH domain containing, RNA binding, signal transduction associated 3
10586368	1.503	Clpx	caseinolytic peptidase X (E.coli)
10372988	1.499	Slc16a7	solute carrier family 16 (monocarboxylic acid transporters), member 7
10371332	1.496	Aldh1l2	aldehyde dehydrogenase 1 family, member L2
10513158	1.496	Ptpn3	protein tyrosine phosphatase, non-receptor type 3
10551393	1.496	LOC100048123///Akt2	thymoma viral proto-oncogene 2
10494085	1.495	Selenbp2	selenium binding protein 2
10405727	1.487	2410127L17Rik	RIKEN cDNA 2410127L17 gene
10412481	1.486	2410127L17Rik	RIKEN cDNA 2410127L17 gene
10529515	1.483	Sorcs2	sortilin-related VPS10 domain containing receptor 2
10587871	1.482	Paqr9	progestin and adipoQ receptor family member IX
10482181	1.481	Strbp	spermatid perinuclear RNA binding protein
10382573	1.479	2310067B10Rik	RIKEN cDNA 2310067B10 gene
10510957	1.478	Pank4	pantothenate kinase 4
10461921	1.477	2410127L17Rik	RIKEN cDNA 2410127L17 gene
10365408	1.476	Ric8b	resistance to inhibitors of cholinesterase 8 homolog B (C. elegans)
10496605	1.468	Ccbl2	cysteine conjugate-beta lyase 2
10501555	1.467	Amy1	amylase 1, salivary
10412909	1.466	Fdft1	farnesyl diphosphate farnesyl transferase 1
10474836	1.465	Ivd	isovaleryl coenzyme A dehydrogenase
10593789	1.454	Etfa	electron transferring flavoprotein, alpha polypeptide
10533345	1.453	Aldh2	aldehyde dehydrogenase 2, mitochondrial
10361926	1.449	Map3k5	mitogen-activated protein kinase kinase kinase 5
10355084	1.448	Ndufs1	NADH dehydrogenase (ubiquinone) Fe-S protein 1
10412882	1.447	Thrb	thyroid hormone receptor beta
10408656	1.445	Peci	peroxisomal delta3, delta2-enoyl-Coenzyme A isomerase
10495562	1.444	Lrrc39	leucine rich repeat containing 39
10420730	1.443	Fdft1	farnesyl diphosphate farnesyl transferase 1
10553935	1.443	Tm2d3///Tarsl2	threonyl-tRNA synthetase-like 2///TM2 domain containing 3
10346365	1.442	Sgol2	shugoshin-like 2 (S. pombe)
10410743	1.441	Ankrd32	ankyrin repeat domain 32
10467162	1.441	Pank1	pantothenate kinase 1

10578810	1.441	Clcn3	chloride channel 3
10511382	1.438	Nsmaf	neutral sphingomyelinase (N-SMase) activation associated factor
10502982	1.436	Tnni3k	TNNI3 interacting kinase
10546129	1.435	Kbtbd12	kelch repeat and BTB (POZ) domain containing 12
10524460	1.435	Acacb	acetyl-Coenzyme A carboxylase beta
10481474	1.433	Crat	carnitine acetyltransferase
10494551	1.433	Acp6	acid phosphatase 6, lysophosphatidic
10455912	1.432	Isoc1	isochorismatase domain containing 1
10497309	1.430	Snx16	sorting nexin 16
10488322	1.430	Ralgapa2	Ral GTPase activating protein, alpha subunit 2 (catalytic)
10420804	1.429	4933401F05Rik	RIKEN cDNA 4933401F05 gene
10492469	1.422	Mlf1	myeloid leukemia factor 1
10443391	1.422	Mapk14	mitogen-activated protein kinase 14
10506154	1.422	Alg6	asparagine-linked glycosylation 6 homolog (yeast, alpha-1,3,-glucosyltransferase)
10399882	1.421	Dus4l	dihydrouridine synthase 4-like (S. cerevisiae)
10346260	1.419	Osgepl1	O-sialoglycoprotein endopeptidase-like 1
10364030	1.418	Adora2a	adenosine A2a receptor
10483521	1.414	Fastkd1	FAST kinase domains 1
10522160	1.413	N4bp2	NEDD4 binding protein 2
10582229	1.412	1110003O08Rik	RIKEN cDNA 1110003O08 gene
10368162	1.409	Pex7	peroxisomal biogenesis factor 7
10511333	1.409	Plag1	pleiomorphic adenoma gene 1
10484207	1.407	2610301F02Rik	RIKEN cDNA 2610301F02 gene
10355343	1.406	Abca12	ATP-binding cassette, sub-family A (ABC1), member 12

Supplemental Table 4 - GO: WT TAC < WT Sham								
GO ID	GO ACCESSION	GO Term	p-value	corrected p-value	Count in Selection	% Count in Selection	Count in Total	% Count in Total
3518	GO:0005739	mitochondrion	5.96E-10	5.24E-06	30	39.473682	1393	6.393721
2134	GO:0003824	catalytic activity	1.92E-09	8.43E-06	34	44.736843	4937	22.660301
3517	GO:0005737	cytoplasm	8.18E-07	0.002398932	60	78.947365	6718	30.834902
5226	GO:0008152	metabolic process	2.90E-06	0.004247454	18	23.68421	6932	31.817139
3552	GO:0005777|GO:0019818	peroxisome	3.93E-06	0.00432228	7	9.210526	102	0.4681691
17438	GO:0042579	microbody	3.93E-06	0.00432228	7	9.210526	102	0.4681691
8779	GO:0016301	kinase activity	1.16E-05	0.009255758	14	18.421053	794	3.644375

Supplemental Table 5 - KO Sham > WT Sham			
Affy ID	**Fold**	**Gene symbol**	**Description**
10481627	2.994	Lcn2	lipocalin 2
10574023	2.379	Mt2	metallothionein 2
10538802	2.323	A930038C07Rik	RIKEN cDNA A930038C07 gene
10398075	2.232	Serpina3n	serine (or cysteine) peptidase inhibitor, clade A, member 3N
10534667	2.011	Serpine1	serine (or cysteine) peptidase inhibitor, clade E, member 1
10416181	1.786	Stc1	stanniocalcin 1
10358476	1.639	Prg4	proteoglycan 4 (megakaryocyte stimulating factor, articular superficial zone protein)
10462442	1.636	Il33	interleukin 33
10555389	1.533	Ucp2	uncoupling protein 2 (mitochondrial, proton carrier)
10450242	1.525	C4b///C4a	complement component 4B (Childo blood group)///complement component 4A (Rodgers blood group)
10566346	1.500	9230105E10Rik	RIKEN cDNA 9230105E10 gene
10598976	1.496	Timp1	tissue inhibitor of metalloproteinase 1
10360985	1.494	Cenpf	centromere protein F
10538082	1.487	Atp6v0e2	ATPase, H+ transporting, lysosomal V0 subunit E2
10601701	1.415	Tmem35	transmembrane protein 35

Supplemental Table 6 - GO: KO Sham > WT Sham								
GO ID	GO ACCESSION	GO Term	p-value	corrected p-value	Count in Selection	% Count in Selection	Count in Total	% Count in Total

No GO lists pass the cut

Supplemental Table 7 - KO Sham < WT Sham			
Affy ID	**Fold**	**Gene symbol**	**Description**
10386197	1.676	2210407C18Rik	RIKEN cDNA 2210407C18 gene
10510260	1.434	Nppb	natriuretic peptide precursor type B

Supplemental Table 8 - GO: KO Sham < WT Sham								
GO ID	GO ACCESSION	GO Term	p-value	corrected p-value	Count in Selection	% Count in Selection	Count in Total	% Count in Total

No GO lists pass the cut

Supplemental Table 9 - KO TAC > KO Sham			
Affy ID	**Fold**	**Gene symbol**	**Description**
10510260	3.008	Nppb	natriuretic peptide precursor type B
10419934	2.866	Myh7	myosin, heavy polypeptide 7, cardiac muscle, beta
10586357	2.733	Cilp	cartilage intermediate layer protein, nucleotide pyrophosphohydrolase
10582592	2.718	Acta1	actin, alpha 1, skeletal muscle
10510265	2.567	Nppa	natriuretic peptide precursor type A
10440091	2.506	Col8a1	collagen, type VIII, alpha 1
10492021	2.336	Postn	periostin, osteoblast specific factor
10541496	2.309	Mfap5	microfibrillar associated protein 5
10376778	2.141	Mfap4	microfibrillar-associated protein 4
10401841	2.027	Dio2	deiodinase, iodothyronine, type II
10448307	2.014	Tnfrsf12a	tumor necrosis factor receptor superfamily, member 12a
10359851	1.989	Uck2	uridine-cytidine kinase 2
10598976	1.943	Timp1	tissue inhibitor of metalloproteinase 1
10484307	1.934	Frzb	frizzled-related protein
10401527	1.880	Ltbp2	latent transforming growth factor beta binding protein 2
10513208	1.835	Svep1	sushi, von Willebrand factor type A, EGF and pentraxin domain containing 1
10435641	1.833	Fstl1	follistatin-like 1
10542355	1.820	Emp1	epithelial membrane protein 1
10359849	1.775	Uck2	uridine-cytidine kinase 2
10554752	1.769	Nox4	NADPH oxidase 4
10417212	1.750	Itgbl1	integrin, beta-like 1
10517213	1.749	Cnksr1	connector enhancer of kinase suppressor of Ras 1
10416215	1.740	Loxl2	lysyl oxidase-like 2
10573979	1.666	Gnao1	guanine nucleotide binding protein, alpha O
10388430	1.637	Serpinf1	serine (or cysteine) peptidase inhibitor, clade F, member 1
10380419	1.624	Col1a1	collagen, type I, alpha 1
10472426	1.623	Xirp2	xin actin-binding repeat containing 2
10407481	1.615	Pfkp	phosphofructokinase, platelet
10490159	1.605	Pmepa1	prostate transmembrane protein, androgen induced 1
10360764	1.601	Enah	enabled homolog (Drosophila)
10573747	1.597	Adcy7	adenylate cyclase 7
10346015	1.575	Col3a1	collagen, type III, alpha 1
10357043	1.562	Bcl2	B-cell leukemia/lymphoma 2
10444591	1.556	Hspa1l	heat shock protein 1-like
10424140	1.553	Col14a1	collagen, type XIV, alpha 1
10548128	1.542	Tspan9	tetraspanin 9
10536220	1.532	Col1a2	collagen, type I, alpha 2
10500295	1.522	Plekho1	pleckstrin homology domain containing, family O member 1
10452485	1.512	Rab31	RAB31, member RAS oncogene family
10455461	1.475	Myot	myotilin
10513739	1.454	Tnc	tenascin C
10355403	1.437	Fn1	fibronectin 1
10445347	1.433	Clic5	chloride intracellular channel 5
10519140	1.430	Mmp23	matrix metallopeptidase 23
10467191	1.428	Ankrd1	ankyrin repeat domain 1 (cardiac muscle)
10381898	1.424	Mrc2	mannose receptor, C type 2
10386058	1.409	Sparc	secreted acidic cysteine rich glycoprotein

Supplemental Table 10 - GO: KO TAC > KO Sham								
GO ID	GO ACCESSION	GO Term	p-value	corrected p-value	Count in Selection	% Count in Selection	Count in Total	% Count in Total
12843	GO:0031012	extracellular matrix	7.22E-16	4.44E-12	14	43.75	292	1.3402488
3396	GO:0005578	proteinaceous extracellular matrix	1.04E-14	3.20E-11	13	40.625	274	1.2576307
3394	GO:0005576	extracellular region	3.52E-14	7.22E-11	23	71.875	1688	7.7477393
18811	GO:0044420	extracellular matrix part	1.65E-13	2.53E-10	8	25	87	0.3993207
18812	GO:0044421	extracellular region part	2.25E-11	2.76E-08	14	43.75	760	3.4883187
4699	GO:0007155	cell adhesion	3.69E-08	3.24E-05	9	28.125	603	2.7677054
11867	GO:0022610	biological adhesion	3.69E-08	3.24E-05	9	28.125	603	2.7677054
3205	GO:0005201	extracellular matrix structural constituent	1.79E-07	1.22E-04	3	9.375	24	0.11015743
3400	GO:0005583	fibrillar collagen	1.75E-07	1.22E-04	2	6.25	6	0.027539358
3351	GO:0005488	binding	2.53E-07	1.55E-04	23	71.875	11058	50.75504
3420	GO:0005604	basement membrane	3.66E-07	2.05E-04	5	15.625	70	0.32129252
22049	GO:0048407	platelet-derived growth factor binding	1.05E-06	5.36E-04	3	9.375	10	0.04589893
3365	GO:0005515|GO:0045308	protein binding	1.77E-06	8.38E-04	21	65.625	5545	25.450956
3401	GO:0005584	collagen type I	4.36E-06	1.92E-03	2	6.25	2	0.009179786
4795	GO:0007275	multicellular organismal development	6.53E-06	0.002508909	4	12.5	2502	11.483912
3398	GO:0005581	collagen	7.03E-06	2.54E-03	3	9.375	18	0.08261807
11152	GO:0019838	growth factor binding	1.61E-05	0.005227941	4	12.5	72	0.3304723

Supplemental Table 11 - KO TAC < KO Sham			
Affy ID	**Fold**	**Gene symbol**	**Description**
10580635	2.246	Ces3	carboxylesterase 3
10602385	2.211	Pfkfb1	6-phosphofructo-2-kinase/fructose-2,6-biphosphatase 1
10598077	1.926		
10511363	1.855	Penk	preproenkephalin
10480459	1.845	Hnmt	histamine N-methyltransferase
10534085	1.804	Phkg1	phosphorylase kinase gamma 1
10441794	1.770	Mrgprh	MAS-related GPR, member H
10397763	1.749	9030617O03Rik	RIKEN cDNA 9030617O03 gene
10606436	1.723	Hmgn5	high-mobility group nucleosome binding domain 5
10386197	1.714	2210407C18Rik	RIKEN cDNA 2210407C18 gene
10419525	1.708	A930018M24Rik	RIKEN cDNA A930018M24 gene
10603746	1.704	Maob	monoamine oxidase B
10574488	1.674	Pdp2	pyruvate dehyrogenase phosphatase catalytic subunit 2
10433177	1.651	Gm9108	predicted gene 9108
10462303	1.648	Kcnv2	potassium channel, subfamily V, member 2
10579958	1.633	Il15	interleukin 15
10369806	1.625	1700040L02Rik	RIKEN cDNA 1700040L02 gene
10428619	1.613	Enpp2	ectonucleotide pyrophosphatase/phosphodiesterase 2
10601701	1.593	Tmem35	transmembrane protein 35
10360985	1.584	Cenpf	centromere protein F
10436095	1.562	Retnla	resistin like alpha
10481627	1.519	Lcn2	lipocalin 2
10512279	1.517	Cntfr	ciliary neurotrophic factor receptor
10433403	1.507	A2bp1	ataxin 2 binding protein 1
10474361	1.505	Mpped2	metallophosphoesterase domain containing 2
10402117	1.497	Rps6ka5	ribosomal protein S6 kinase, polypeptide 5
10377245	1.495	Dhrs7c	dehydrogenase/reductase (SDR family) member 7C
10536611	1.493	Kcnd2	potassium voltage-gated channel, Shal-related family, member 2
10466903	1.489	4430402I18Rik	RIKEN cDNA 4430402I18 gene
10372988	1.488	Slc16a7	solute carrier family 16 (monocarboxylic acid transporters), member 7
10348906	1.486	Gm6086	predicted gene 6086
10409999	1.481	Fbp2	fructose bisphosphatase 2
10409118	1.478	Wnk2	WNK lysine deficient protein kinase 2
10544687	1.478	Cycs	cytochrome c, somatic
10413381	1.473	Dnahc12///Asb14	dynein, axonemal, heavy chain 12///ankyrin repeat and SOCS box-containing 14
10423505	1.468	Cmbl	carboxymethylenebutenolidase-like (Pseudomonas)
10422962	1.467	1110020G09Rik	RIKEN cDNA 1110020G09 gene
10412909	1.459	Fdft1	farnesyl diphosphate farnesyl transferase 1
10532085	1.453	Tgfbr3	transforming growth factor, beta receptor III
10545001	1.451	Ppm1k	protein phosphatase 1K (PP2C domain containing)
10398824	1.447	A530016L24Rik	RIKEN cDNA A530016L24 gene
10575363	1.445	Zfp612	zinc finger protein 612
10592061	1.444	Kcnj5	potassium inwardly-rectifying channel, subfamily J, member 5
10537712	1.443	Gstk1	glutathione S-transferase kappa 1
10344725	1.435	Adhfe1	alcohol dehydrogenase, iron containing, 1
10495675	1.435	F3	coagulation factor III
10396079	1.434	Klhdc1	kelch domain containing 1
10501208	1.432	Gstm6	glutathione S-transferase, mu 6
10601844	1.431	Bhlhb9	basic helix-loop-helix domain containing, class B9
10357965	1.430	Lgr6	leucine-rich repeat-containing G protein-coupled receptor 6
10582229	1.430	1110003O08Rik	RIKEN cDNA 1110003O08 gene
10494114	1.426	Selenbp1///Selenbp2///L	selenium binding protein 2///hypothetical protein LOC100044204///selenium binding
10494085	1.424	Selenbp2	selenium binding protein 2
10386020	1.418	Slc36a2	solute carrier family 36 (proton/amino acid symporter), member 2

Supplemental Table 12 - GO: KO TAC < KO Sham								
GO ID	GO ACCESSION	GO Term	p-value	corrected p-value	Count in Selection	% Count in Selection	Count in Total	% Count in Total

No GO lists pass the cut

Supplemental Table 13 - KO TAC > WT TAC			
Affy ID	**Fold**	**Gene symbol**	**Description**
10580635	3.370	Ces3	carboxylesterase 3
10538802	2.322	A930038C07Rik	RIKEN cDNA A930038C07 gene
10598064	2.276		
10598018	2.188		
10598062	1.880		
10511363	1.874	Penk	preproenkephalin
10441794	1.676	Mrgprh	MAS-related GPR, member H
10478145	1.550	Ppp1r16b	protein phosphatase 1, regulatory (inhibitor) subunit 16B
10398824	1.541	A530016L24Rik	RIKEN cDNA A530016L24 gene
10468113	1.538	Kcnip2	Kv channel-interacting protein 2
10497862	1.520	Trpc3	transient receptor potential cation channel, subfamily C, member 3
10598023	1.517		
10601878	1.501	Tceal1	transcription elongation factor A (SII)-like 1
10542834	1.486		
10534085	1.471	Phkg1	phosphorylase kinase gamma 1
10352133	1.440	Efcab2	EF-hand calcium binding domain 2
10574488	1.429	Pdp2	pyruvate dehyrogenase phosphatase catalytic subunit 2
10397763	1.408	9030617O03Rik	RIKEN cDNA 9030617O03 gene

Supplemental Table 14 - GO: KO TAC > WT TAC								
GO ID	GO ACCESSION	GO Term	p-value	corrected p-value	Count in Selection	% Count in Selection	Count in Total	% Count in Total

No GO lists pass the cut

Supplemental Table 15 - KO TAC < WT TAC			
Affy ID	**Fold**	**Gene symbol**	**Description**
10398075	3.851	Serpina3n	serine (or cysteine) peptidase inhibitor, clade A, member 3N
10572897	3.263	Hmox1	heme oxygenase (decycling) 1
10358476	2.822	Prg4	proteoglycan 4 (megakaryocyte stimulating factor, articular superficial zone protein)
10492021	2.784	Postn	periostin, osteoblast specific factor
10462442	2.741	Il33	interleukin 33
10416181	2.681	Stc1	stanniocalcin 1
10598976	2.637	Timp1	tissue inhibitor of metalloproteinase 1
10481627	2.441	Lcn2	lipocalin 2
10574023	2.394	Mt2	metallothionein 2
10355403	2.353	Fn1	fibronectin 1
10401527	2.168	Ltbp2	latent transforming growth factor beta binding protein 2
10475517	2.125	AA467197	expressed sequence AA467197
10513739	2.108	Tnc	tenascin C
10419934	2.067	Myh7	myosin, heavy polypeptide 7, cardiac muscle, beta
10586357	2.006	Cilp	cartilage intermediate layer protein, nucleotide pyrophosphohydrolase
10478048	1.918	Lbp	lipopolysaccharide binding protein
10376778	1.864	Mfap4	microfibrillar-associated protein 4
10523175	1.834	Ereg	epiregulin
10463070	1.831	Entpd1	ectonucleoside triphosphate diphosphohydrolase 1
10380419	1.828	Col1a1	collagen, type I, alpha 1
10440091	1.827	Col8a1	collagen, type VIII, alpha 1
10541496	1.820	Mfap5	microfibrillar associated protein 5
10424140	1.816	Col14a1	collagen, type XIV, alpha 1
10534667	1.788	Serpine1	serine (or cysteine) peptidase inhibitor, clade E, member 1
10429128	1.768	Sla	src-like adaptor
10586865	1.744	Aldh1a2	aldehyde dehydrogenase family 1, subfamily A2
10434698	1.740	Fetub	fetuin beta
10425066	1.731	Csf2rb	colony stimulating factor 2 receptor, beta, low-affinity (granulocyte-macrophage)
10494271	1.721	Ctss	cathepsin S
10435641	1.709	Fstl1	follistatin-like 1
10536220	1.689	Col1a2	collagen, type I, alpha 2
10461721	1.684	Mpeg1	macrophage expressed gene 1
10354003	1.684	Mgat4a	mannoside acetylglucosaminyltransferase 4, isoenzyme A
10422164	1.662	Ednrb	endothelin receptor type B
10416215	1.659	Loxl2	lysyl oxidase-like 2
10409464	1.651	Dbn1	drebrin 1
10417212	1.626	Itgbl1	integrin, beta-like 1
10360028	1.620	Fcgr2b	Fc receptor, IgG, low affinity IIb
10542355	1.604	Emp1	epithelial membrane protein 1
10365482	1.600	Timp3	tissue inhibitor of metalloproteinase 3
10484307	1.599	Frzb	frizzled-related protein
10462005	1.592	Tmem2	transmembrane protein 2
10526514	1.584	Cldn15	claudin 15
10586246	1.581	Dennd4a	DENN/MADD domain containing 4A
10374083	1.580	Aebp1	AE binding protein 1
10346015	1.577	Col3a1	collagen, type III, alpha 1
10359851	1.575	Uck2	uridine-cytidine kinase 2
10555389	1.565	Ucp2	uncoupling protein 2 (mitochondrial, proton carrier)
10596747	1.544	Sema3f	sema domain, immunoglobulin domain (Ig), short basic domain, secreted, (semaphorin) 3F
10517213	1.520	Cnksr1	connector enhancer of kinase suppressor of Ras 1
10494262	1.516	Ctsk	cathepsin K
10398052	1.505	Serpina3h	serine (or cysteine) peptidase inhibitor, clade A, member 3H
10388430	1.496	Serpinf1	serine (or cysteine) peptidase inhibitor, clade F, member 1
10401244	1.489	Actn1	actinin, alpha 1
10401781	1.478	Sptlc2	serine palmitoyltransferase, long chain base subunit 2
10513208	1.476	Svep1	sushi, von Willebrand factor type A, EGF and pentraxin domain containing 1
10604961	1.474	Gabra3	gamma-aminobutyric acid (GABA) A receptor, subunit alpha 3

10527233	1.454	Cyth3	cytohesin 3
10464761	1.447	Syt12	synaptotagmin XII
10467420	1.433	Pdlim1	PDZ and LIM domain 1 (elfin)
10582275	1.432	Slc7a5	solute carrier family 7 (cationic amino acid transporter, y+ system), member 5
10607870	1.431	Tlr7	toll-like receptor 7
10459421	1.415	Atp8b1	ATPase, class I, type 8B, member 1
10510265	1.410	Nppa	natriuretic peptide precursor type A
10373902	1.409	Gatsl3	GATS protein-like 3
10371321	1.406	Slc41a2	solute carrier family 41, member 2
10528268	1.405	Ptpn12	protein tyrosine phosphatase, non-receptor type 12

Supplemental Table 16 - GO: KO TAC < WT TAC								
GO ID	GO ACCESSION	GO Term	p-value	corrected p-value	Count in Selection	% Count in Selection	Count in Total	% Count in Total
3394	GO:0005576	extracellular region	1.10E-21	7.20E-18	34	100	1688	7.7477393
3396	GO:0005578	proteinaceous extracellular matrix	9.58E-14	2.73E-10	13	38.235294	274	1.2576307
18811	GO:0044420	extracellular matrix part	1.25E-13	2.73E-10	8	23.529411	87	0.3993207
12843	GO:0031012	extracellular matrix	2.29E-13	3.76E-10	13	38.235294	292	1.3402488
18812	GO:0044421	extracellular region part	8.18E-13	1.07E-09	13	38.235294	760	3.4883187
3420	GO:0005604	basement membrane	7.56E-08	8.27E-05	5	14.705882	70	0.32129252
3400	GO:0005583	fibrillar collagen	5.52E-07	5.18E-04	2	5.882353	6	0.027539358
3205	GO:0005201	extracellular matrix structural constituent	8.29E-07	6.80E-04	3	8.823529	24	0.11015743
22049	GO:0048407	platelet-derived growth factor binding	3.28E-06	0.002329905	3	8.823529	10	0.04589893
12309	GO:0030414	protease inhibitor activity	4.96E-06	2.96E-03	2	5.882353	142	0.6517648
3401	GO:0005584	collagen type I	9.32E-06	5.10E-03	2	5.882353	2	0.009179786

Table S17

Target Protein	*Number of hits*
Syntenin	34
Connective tissue growth factor (CTGF)	14
Granulin	12
EGF-containing fibulin-like extracellular matrix protein 2 (EFEMP2	11
Fibronectin 1	5
Dickkopf homolog 3 (DKK3)	4
Laminin gamma 1	4
Latent transforming growth factor beta binding protein 2 (LTBP2)	4
Proprotein convertase subtilisin/kexin type 6	3
NUFIP2	2
Laminin beta 2	1
Sorting nexin 3 (SNX3)	1
Y box binding protein 1 (YBX1)	1
CD63 antigen	1
Fibulin 5	1
Fibulin 2	1
Cyclophilin D	1
Ribophorin 1	1
Sprouty homolog 2	1
ZNF 330	1
Rabin 3	1
Lactate dehydrogenase A	1
NDRG 4	1
Ceramide synthase 2	1
Fibrillin 1	1
HLA-B associated transcript 1	1
Thrombospondin 1	1
Total	110